Single Cell RT-qPCR on 3D Cell Spheroids

by

Kuo-chen Wang

A Dissertation Presented in Partial Fulfillment
of the Requirements for the Degree
Doctor of Philosophy

Approved November 2016 by the
Graduate Supervisory Committee:

Deirdre R. Meldrum, Chair
Shih-hui Chao
Hong Wang
Michael Goryll

ARIZONA STATE UNIVERSITY

December 2016

ABSTRACT

A single cell is the very fundamental element in an organism; however, it contains the most complicated and stochastic information, such as DNA, RNA, and protein expression. Thus, it is a necessity to study stochastic gene expression in order to discover the biosignatures at the single-cell level. The heterogeneous gene expression of single cells from an isogenic cell population has already been studied for years. Yet to date, single-cell studies have been confined in a fashion of analyzing isolated single cells or a dilution of cells from the bulk-cell populations. These techniques or devices are limited by either the mechanism of cell lysis or the difficulties to target specific cells without harming neighboring cells.

This dissertation presents the development of a laser lysis chip combined with a two-photon laser system to perform single-cell lysis of single cells *in situ* from three-dimensional (3D) cell spheroids followed by analysis of the cell lysate with two-step reverse transcription-quantitative polymerase chain reaction (RT-qPCR). The 3D spheroids were trapped in a well in the custom-designed laser lysis chip. Next, each single cell of interest in the 3D spheroid was identified and lysed one at a time utilizing a two-photon excited laser. After each cell lysis, the contents inside the target cell were released to the surrounding media and carried out to the lysate collector. Finally, the gene expression of each individual cell was measured by two-step RT-qPCR then spatially mapped back to its original location in the spheroids to construct a 3D gene expression map.

This novel technology and approach enables multiple gene expression measurements in single cells of multicellular organisms as well as cell-to-cell heterogeneous responses to the environment with spatial recognition. Furthermore, this

method can be applied to study precancerous tissues for a better understanding of cancer progression and for identifying early tumor development.

Dedicated

to

My Parents, CP Wang and May Liu

My Brother, Kuo Wang

and My lovely Wife, Xiaomei Ma

ACKNOWLEDGMENTS

There are so many people I have to thank for helping me get to where I am today. I owe my gratitude to many people who inspired me and helped me through these years at Arizona State University.

First and foremost, I would like to express my deep and sincere gratitude to my advisor and committee chair, Dr. Deirdre Meldrum, for accepting me as her student and supporting me in every possible manner during my studies. I am very grateful that she gave me this great opportunity to work on this research at the Center of Biosignatures Discovery Automation at Arizona State University. I am very fortunate to have her as my advisor without whom I could not have my current achievement.

I am greatly indebted to Dr. Shih-hui Chao. For his invaluable day-to-day mentorship and guiding me throughout the whole doctoral study. In addition to his mentorship, he has given me the intellectual freedom to develop various approaches related to this work. Furthermore, he also gives me many useful advice for both professionally and personally. It is a truly pleasure to work with him during my doctoral journey.

I am extremely thankful to Dr. Hong Wang, who led me into this lab and always supported and advised me in every possible ways. He is not only given time and effort helping my writing, but also mentoring me regards to fabrication knowledge. I am very thankful to his help, I could not be in this position without him.

I would like to thank Professor Michael Goryll who served as my dissertation committee member. For his patience, kindness, time and gave me a lot of helpful suggestions that greatly improved this work. This work could not have been completed without the input and collaboration from him.

Special thanks to Dr. Weimin Gao, for all the support and mentor regards to biology techniques and knowledge. Without his help, this dissertation could not complete. Also I would like to acknowledge all the CBDA members include Dr. Laimonas Kelbauskas, Dr. Honor Glenn, Dr. Yanqing Tian, Dr. Fengyu Su, Dr. Liqing Zhang, Dr. Xiangxing Kong, Dr. Bin Cao, Carol Glaub, Christine Willett, Morgan Bennett, Jeff Houkal, specifically Sandhya Gangaraju for cell culturing help, Juan Vela for CNC fabrication, Dean Smith for software programming, and all the staff from CSSER. I thank all of my colleagues, Ganquan, Shufang, Rishabh, and Meryl for all the support and time they gave me in CBDA.

For my family, there is no word that I can describe my gratitude to them. I owe my entire life to my parents. None of my achievements could be done without their selfless dedication and sacrifices. At last, I would like to express my deepest gratitude to my lovely and amazingly wife. She is always there to encourage me when things going wrong and providing constant care to me all the way to the finish line. Her endless support and encouragement have been monumental during this journey. This accomplishment could not done without her. Thank you, Xiaomei.

TABLE OF CONTENTS

Page

CHAPTER Page

CHAPTER Page

LIST OF TABLES

Table Page

LIST OF FIGURES

Figure Page

Figure Page

1. INTRODUCTION

1.1 Motivation

Cellular heterogeneity in an isogenic population has been revealed for decades (Spudich and Koshland 1976), but how to measure and analyze these heterogeneities has become an imperative for single-cell analysis. Most single-cell studies focus on dispersed cell populations, whereas only a few of them measure cellular characteristics in the context of tissue or multicellular systems. For example, fluorescence *in situ* hybridization (FISH) uses imaging techniques to measure cellular genetic variation (Levsky et al. 2002). Another example is a fluorophore-based barcoding approach with optical super-resolution microscopy (Lubeck and Cai 2012). However, both approaches have their limitation. FISH can only examine a small number of gene expressions which becomes a huge problem for multiplexing. The barcoding method, on the other hand, has increased the capacity for multiplexing detection, but it requires super-resolution microscopy which limits the accessibility for users. To overcome the limitations of cellular analysis in complex biological environments requires the development of single-cell analysis *in situ* in 3D cell spheroids with spatial recognition.

1.2 Approach

This dissertation is motivated by the idea of measuring and analyzing cellular RNA heterogeneity *in situ* in whole organisms or multicellular environments, as well as using these measurements to differentiate specific cell lines in multicellular environments. This dissertation develops a platform that combines a microfluidic device with a two-photon laser lysis system to analyze single-cell gene expression *in situ* in 3D cell clusters. The

concept is to lyse single cells on 3D cell clusters consecutively, conduct RT-qPCR to analyze the mRNA from each individual cell and trace back to the pre-lysis 3D location of the cell in the cell cluster to produce a 3D spatial map of gene expression with single-cell resolution.

The experimental design of this dissertation is described in Figure 1. The laser lysis chip is fabricated using soft lithography techniques. The cell clusters are cultured from a bulk cell population then loaded into the laser lysis chip. The single-cell laser lysis is performed on the cell clusters and the lysate is collected and analyzed by two-step RT-qPCR analysis at the single-cell level. The results are analyzed and compared with different gene expression patterns in order to construct a 3D mRNA map of each cell in the cell cluster.

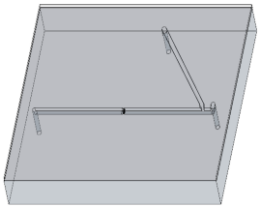

(a)

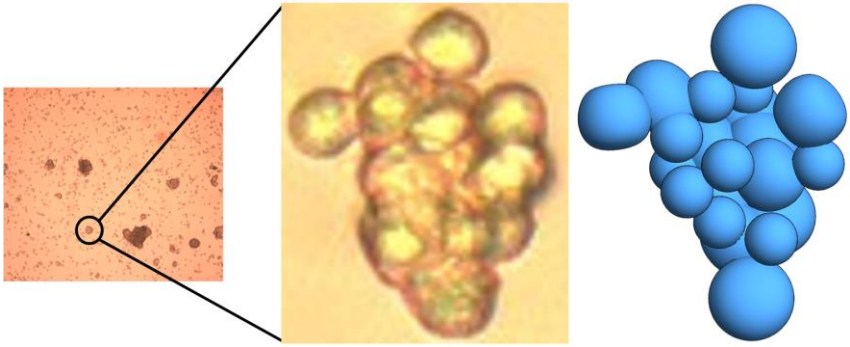

(b)

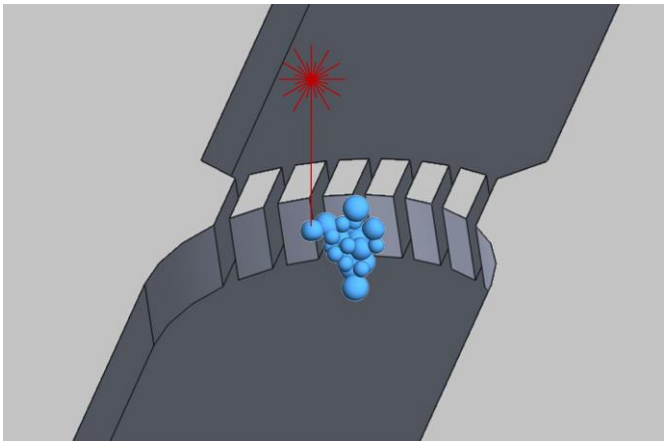

(c)

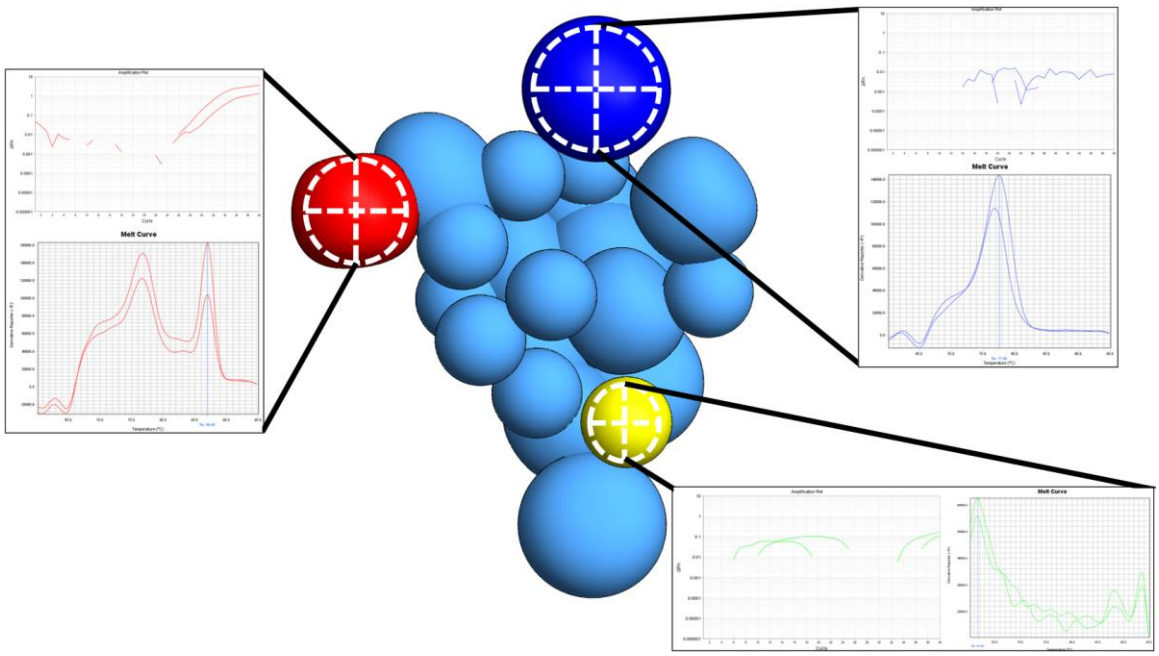

(d)

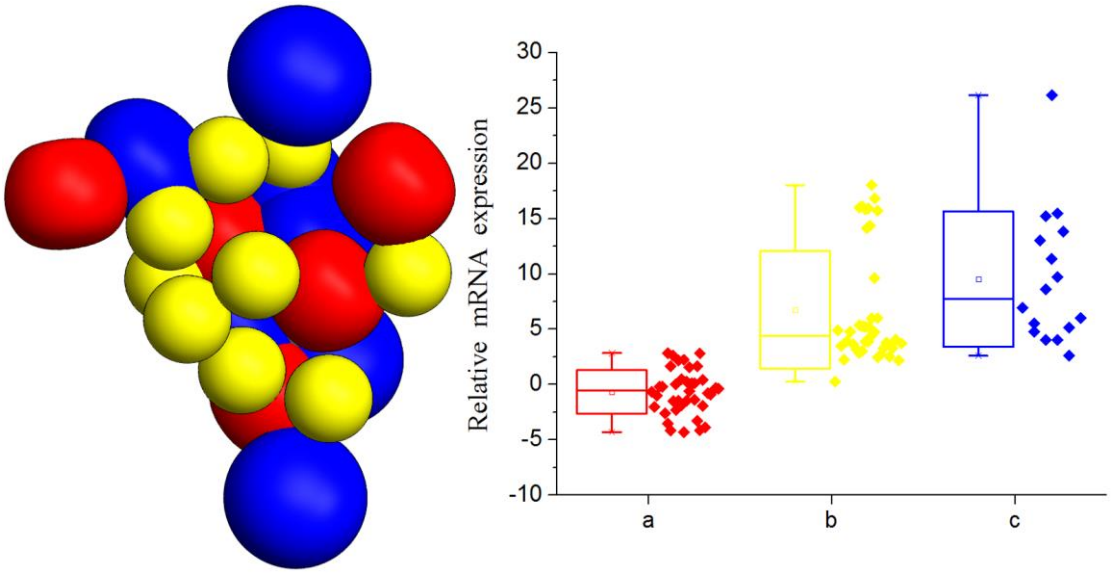

(e)

Figure 1. Schematic Description of Single-cell Analysis *In Situ* 3D Cell Spheroids. (a) Laser lysis chip fabrication. (b) Cell clusters cultivation. (c) Cell clusters trapping and lysing. (d) Single cell laser lysis and gene expression analysis. (e) Data analysis for 3D mRNA mapping.

1.3 Objectives

A platform was developed to study mRNA expressions at the single-cell level and construct a 3D mRNA map with spatial information *in situ* in 3D cell clusters. The objectives of this dissertation are:

i) Design and develop a microfluidic chip for capturing 3D cell spheroids combined with a two-photon laser system to perform single-cell lysis in their in situ environment. This objective includes development of the fabrication process of the laser lysis chip and the principle of the laser lysis method to perform single-cell laser lysis analysis.

ii) Develop and optimize the laser lysis chip system with different approaches. This objective not only validates the mRNA recover efficiency and induced cellular stress of the laser lysis method, but also characterizes the collection process of the laser lysis system.

iii) Analyze the single-cell gene expression patterns on CP-D cell clusters by utilizing the column-based two-step RT-qPCR analysis. This objective shows the laser lysis system can discover gene expression with high sensitivity and specificity at the single-cell level in 3D cell spheroids.

iv) Analyze the single-cell gene expression patterns on mixed CP-D, EPC2 cell clusters, then differentiate cell lines by the distinct expression of an endogenous gene. This objective validates that the system is capable of distinguishing different cell types in multicellular systems.

1.4 Scientific contributions

The major contributions of this dissertation include the following. Firstly, a laser lysis chip was designed and developed to perform laser lysis on 3D cell spheroids at the single-cell level. This device combined with a two-photon laser system provides an enabling technology to lyse individual cells *in situ* in 3D clusters and perform downstream RT-qPCR analysis at the single-cell level. The significance of the laser lysis chip is: a) the released lysates will be carried by surrounding media to the outlet while the cell clusters will be trapped at the cage. This approach allows the laser lysis chip to lyse single cells and collect the lysates sequentially; b) the lysing range can penetrate deeper into the cell clusters by using a two-photon laser system, which will enable the laser lysis to lyse 3D structure cells; c) the system is capable of trapping multiple cell clusters with more than one cell line, and performing laser lysis at the single-cell level.

Secondly, the gene expression patterns *in situ* in 3D CP-D cell clusters were discovered. Many other single-cell studies have focused on scatter and dispersed single cells, but only a few of them have studied 3D cell clusters or defined tissues. This study provides a solution to study single-cell gene expression *in situ* in 3D cell clusters while maintaining its spatial recognition. At the same time, this study also discovers the stochastic gene expressions in dysplasia cultured tissues which will improve single-cell analysis to another level.

Thirdly, this dissertation shows that the laser lysis approach can not only analyze cellular heterogeneity but also differentiate specific cell lines in multicellular environments. In the mixture CP-D and EPC2 cell clusters experiment, the CP-D cell line was discriminated by the endogenous gene expression patterns at the single-cell level. The

differences in the endogenous gene expressions can be used to distinguish different cell types from the mixture-cell clusters. The results demonstrate that this technology can not only work with single-cell line cell clusters, but also apply to multicellular tissues. Complex biological systems can then be studied with 3D gene expression mapping. This study provides a great tool to analyze cellular variation *in situ* in whole organisms or defined tissues for improving prognosis of premalignant conditions.

With these results, and multiple contributions, one manuscript is in preparation for publication, one conference paper was published, and I am an author in several co-author publications.

1. Kuo-chen Wang, Ganquan Song, Yanqing Tian, Shih-Hui Chao, Hong Wang, Deirdre Meldrum. Micropatterning of Cells into Microwells for Metabolic Profiling. *IEEE EMBS Micro and Nanotechnology in Medicine Conference*. 2014. (Conference)
2. Single cell RT-qPCR analysis *in situ* of 3D cell clusters. *In preparation*.

Co-author:

3. Ganquan Song, Kuo-chen Wang, Benjamin Ueberroth, Fred Lee, Liqiang Zhang, Fengyu Su, Haixin Zhu, Qian Mei, Shih-hui Chao, Laimonas Kelbauskas, Yanqing Tian, Hong Wang, Deirdre Meldrum. Single cell metabolic profiling using multiplexed, photo-patterned fluorescence sensor arrays. *18th International Conference on Miniaturized Systems for Chemistry and Life Sciences. Microtas,* pp. 884–886, 2014. (Conference)
4. Jordan Yaron, Jieying Pan, Tejas Borkar, Kristen Lee, Kuo-Chen Wang, Clifford Anderson, Honor Glenn, Deirdre Meldrum. Automated Cell Counting in a High

Density, Polymer-Coated, Live Single Cell Sandwich Microarray. *Microscopy and Microanalysis*, vol. 20, no. S3, pp. 1438–1439, 2014. (Conference)

5. Laimonas Kelbauskas, Rishabh Shetty, Bin Cao, Kuo-chen Wang, Dean Smith, Hong Wang, Joseph Chao, Brian Ashcroft, Margaret Kritzer, Honor Glenn, Roger Johnson, Deirdre Meldrum. Computed tomography for quantitative imaging of live cancer cells with isotropic 3D spatial resolution. *Engineering and Physical Sciences in Oncology*. 2016. (Poster)
6. Laimonas Kelbauskas, Rishabh Shetty, Bin Cao, Kuo-chen Wang, Dean Smith, Hong Wang, Joseph Chao, Brian Ashcroft, Margaret Kritzer, Honor Glenn, Roger Johnson, Deirdre Meldrum. Computed tomography of living single cells in suspension to achieve isotropic 3D spatial resolution for orientation independent measurement. *Under review*.

1.5 Dissertation overview

Chapter 2 provides an overview of *in situ* single-cell analysis, cell lysis introduction, and single cell gene expression analysis. Chapter 3 describes the lysis sample, the Barrett's esophagus cell line, with cell cultivation detail and the target genes selection and validation. Chapter 4 details the design and fabrication processes of the laser lysis chip. Chapter 5 covers different experimental designs for characterization and validation of the laser lysis system in terms of efficiency and contamination issues. This chapter includes analysis of cellular stress and mRNA retrieval efficiency. Chapter 6 shows the single-cell lysis and analysis in CP-D cell clusters experiment and reports the result with housekeeping gene expression levels. Chapter 7 shows the single-cell lysis and analysis *in situ* in mixture CP-

D and EPC2 cell clusters experiment and reports the result with endogenous gene expression patterns. This chapter also describes different sample applications of laser lysis chip. Chapter 8 concludes this dissertation and suggests an outlook on potential future research directions.

2. BACKGROUND LITERATURE

2.1 *In situ* single-cell analysis

In situ single-cell analysis means the analysis of individual cells in a large context of tissue or a multicellular cluster that maintains the original structural and functional characteristics of the native microenvironment. Many single-cell studies have focused on using microfluidics to analyze dispersed single cells, such as manipulation of single cells (Anis, Holl, and Meldrum 2010), gene expression of microbial cells (Gao, Zhang, and Meldrum 2011), array cultivation device for single-cell analysis (Carlo, Wu, and Lee 2006), droplet barcoding single-cell transcription (Klein et al. 2015), and dispersed single cells analysis from cell cluster formation (Chung, Kim, and Yoon 2011; Chen et al. 2016). However, hardly any of these studies analyze single cells *in situ* in a whole tissue that preserves the original characteristics. A few studies have tried using different approaches to study *in situ* single cells, including mRNAs labeling with fluorescence *in situ* hybridization (FISH) (Amann and Fuchs 2008; Lubeck and Cai 2012; Lubeck et al. 2014), computational model development for single-cell RNA sequencing (Fan et al. 2016), and expansion microscopy of cells by labeling with fluorescent proteins and antibodies (Tillberg et al. 2016). Lubeck and Cai (2012) propose to use super-resolution microscopy to observe target molecules attached with fluorophore-based barcodes. This combination method of labeling and super-resolution imaging can be applied to many types of molecules *in situ* and therefore used to study genomics at the single-cell level. Fan et al. (2016) develop pathway and gene set overdispersion analysis to identify sub-populations of mouse neural progenitor cells by reducing technical noises and extra variances in single-cell RNA sequencing. Another new approach, protein retention expansion microscopy, is reported by Tillberg et al. (2016).

This method preserves target proteins in a swollen gel so it can be detected during the expansion process. However, it is still limited in multiplexing measurements.

In short, considering the aforementioned studies and developments of single-cell analysis *in situ* in whole organisms, it would be of great scientific value to further study cellular genetic heterogeneity and define particular cell lines *in situ* in a multicellular cluster or defined tissue.

2.2 Cell lysis introduction

How to lyse the isolated single cells is a crucial task considering the dimension of single cells and the difficulty in lysate collection. Different lysis methods have been developed for particular purposes of single-cell analysis. Here, two commonly used lysis methods, chemical lysis and laser lysis, are illustrated in detail as follows.

2.2.1 Chemical lysis

Chemical lysis, also known as detergent lysis, is a solution-based lysis method using the lysis buffer solution to create pores within cell membranes and thus break up cell structures to lyse cells. Different surfactants like sodium dodecyl sulphate and Triton X-100, are added into lysis buffer in order to speed up cell lysis and increase protein extraction efficiency. The chemical lysis has been widely used not only in bulk-cell populations, but also in the microwell arrays of isolated single cells. Additionally, the solution-based chemical lysis works perfectly on both adherent and suspended cells. Several applications have been developed for single cells, e.g. Shoemaker *et al.* (2005) used the micropipette to transport single cells into a micro-reactor vessel to perform single-cell analysis (Shoemaker

et al. 2005). Ocvirk *et al.* (2004) used a Y-shaped microfluidic device to performed on-chip mixing and lysis of single cells by introducing single cells and lysis buffer at the same time (Ocvirk et al. 2004). Moreover, Huang et al. (2007) elevated chemical lysis application to another level. They designed a microfluidic device with several valves that could trap single cells in chambers and lyse, label, separate, and quantify the protein contents at the single-cell level. Recent studies and current technology (Fluidigm C1™) also utilize the chemical lysis method with the hydrodynamic trapping approach to study single cells (Chen et al. 2016).

2.2.2 Laser lysis

Laser lysis is an application that uses laser pulses to either shoot directly on the target cell or generate a shock wave which creates a cavitation bubble that disrupts the cells. Several applications have been developed, including Rau *et al.* (2004) showed using laser-induced bubbles to lyse cells during a bubble expanding process (Rau et al. 2004; Rau et al. 2006). Hellman *et al.* (2008) categorized three different lysis outcomes: (a) immediate cell lysis; (b) necrotic cell with blebbing membrane; (c) cell poration, by adjusting the distance between the laser focal point and the target cell (Hellman et al. 2008). Furthermore, Quinto-Su *et al*. (2008) recorded and analyzed laser lysis progression in a Poly (dimethylsiloxane) (PDMS) microfluidic channel using time-resolved imaging (Quinto-Su et al. 2008). The result showed laser lysis is advantageous for lab on a chip applications since it does not require complicated instruments and the laser can approach any optically-accessible locations.

Another laser lysis technique is using a two-photon excited laser to perform single-cell lysis. Two-photon excited laser (2PEL) has been widely used on imaging microscopy for it overcomes the limitation of light-scattering issue in large depth biological tissues (Helmchen and Denk 2005). 2PEL has two major advantages: firstly, it utilizes two longer wavelength photons to reach an excitation energy state, instead of using only one-photon excitation which requires a shorter wavelength and higher energy photon (Figure 2a). The two-photon absorption then occurs at the near-infrared region, and is therefore less phototoxic to tissues (Svoboda and Block 1994). Secondly, the excitation intensity of two-photon only appears at a focal point and decreases rapidly out of focal planes. The localized excitation in 2PEL is quite different from single-photon excitation which remains constant throughout the spatial confinement. These results from the 2PEL require two photons to arrive simultaneously which means fluorescence intensity depends on the square of the excitation intensity (Figure 2b) (Soeller and Cannell 1999). Moreover, the absence of out-of-focus planes excitation reduces photobleaching and prolongs tissue viability (Squirrell et al. 1999; Helmchen and Denk 2005).

The cell lysis occurs when the light intensity is increased to 10^{12} W/cm^2. This amount of intensity is sufficient enough to induce ionization and generate free-electrons, resulting in plasma formation. However, there are some destructive effects that need to be resolved under this circumstance. By decreasing the duration of laser pulses from nanosecond to femtosecond greatly reduces the destructive mechanism (Vogel et al. 1999). To acquire 2PEL, a titanium sapphire laser with 800 nm wavelength (Mira 900, Coherent, Santa Clara, CA) is used to produce 150-200 femtosecond pulses at a repetition rate of 250 KHz (RegA, Coherent) with 0.4 μJ pulse energy, and ~1 s total exposure time. A

programmed shutter (SH05 Optical Beam Shutter, Thorlabs, Newton, NJ) is placed on the path of laser to control the numbers of laser pulses sent to the cell.

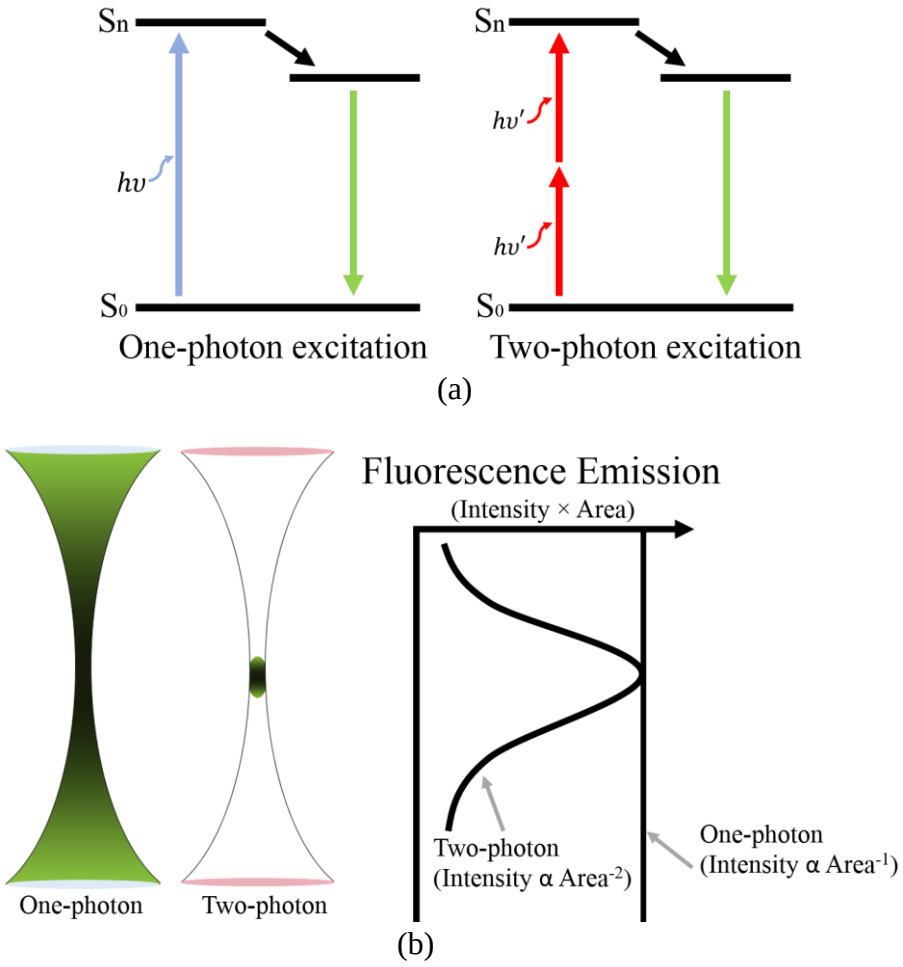

Figure 2. Two-photon Excited Laser Working Theory. (a) Jablonski diagram of single-photon and two-photon excitation comparison. Single-photon requires larger energy to reach excited state while two-photon only needs two photons with less energy. (b) Fluorescence emission difference between single-photon and two-photon excitation. The fluorescence signal is proportional to spatial confinement and photon intensity. Due to the intensity difference between single and two-photon. The emission in two-photon excitation only has peak in focal point and degrades out-of-focus planes, while single-photon stays constant. Images adapted from (Soeller and Cannell 1999).

2.3 Single-cell gene expression analysis

Gene expression analysis at the single-cell level requires higher specificity and sensitivity since it is a known fact that there is stochastic gene expression at the single-cell level in an isogenic cell population. There are a lot of factors causing the cell-to-cell heterogeneity, including biological noises, genetic properties, and regulatory fluctuation (Banerjee et al. 2004; Colman-Lerner et al. 2005; Pedraza and Oudenaarden 2005; Rosenfeld et al. 2005; Newman et al. 2006; Strovas et al. 2007). Therefore, the genetic properties including RNA, DNA, and proteins may contain different copy numbers at the single-cell level. How to analyze the gene expression at the single-cell level becomes a critical part to study single cells.

Single-cell studies have been under development for a long time and numerous methods have been proposed to analyze single-cell gene expression (Le et al. 2006; Cai, Friedman, and Xie 2006; Yu et al. 2006; Strovas et al. 2007; Stewart and Franklin 2008; Guet et al. 2008). The most notable method is utilizing green fluorescent protein (GFP) as a marker to study gene expression (Chalfie et al. 1994). Other protocols use different mechanisms, such as luciferase (Wet et al. 1987; Gould and Subramani 1988; Hoshino, Nakajima, and Ohmiya 2007), amino acid trapping approach with protein (Zhao et al. 2013; Zhao et al. 2014; Lindsay, Zhang, and Zhao 2015), fluorescence *in situ* hybridization (FISH) (Moter and Göbel 2000; Levsky and Singer 2003; Pernthaler and Amann 2004; Amann and Fuchs 2008), and reverse transcription polymerase chain reaction (RT-PCR) (Bustin 2000; Bustin et al. 2005). Among all approaches, RT-PCR is the most sensitive technique that can detect and quantitate mRNA even at the single-cell level (Kubista et al. 2006; Nolan, Hands, and Bustin 2006). Multiple reports demonstrate how to utilize RT-qPCR for

mRNA quantification and analysis of the genetic expression in single cells (Lindqvist, Vidal-Sanz, and Hallböök 2002; Marcus, Anderson, and Quake 2006; Hartshorn et al. 2007; Wacker, Tehel, and Gallagher 2008; Li et al. 2010; Gao, Zhang, and Meldrum 2011).

A two-step SYBR Green-based single-cell RT-qPCR method was developed to measure gene expression directly in *Escherichia coli* populations (Gao, Zhang, and Meldrum 2011). This method can measure multiple gene expressions simultaneously at the single-cell level. The first step is RNA isolation from a single cell and cDNA synthesis. The second step is qPCR process which determines expression levels of multiple genes simultaneously in one single cell. The result showed that this method not only can measure cellular variations with high sensitivity at the single-cell level but also can reproducibly measure multiple gene expressions from one single cell. In short, this method is advantageous for single-cell analysis owing to it can measure multiple gene expression patterns at the single-cell level with high accuracy and cost-efficiency.

3. BARRETT'S ESOPHAGUS CELL LINE

3.1 Barrett's esophagus

Barrett's esophagus (BE) is a condition of the normal tissue in the esophagus being replaced by tissue similar to the intestine lining. The cause of BE is from the backing up of stomach contents (acid reflux) that may irritate the esophagus and, over time, cause BE. People with BE are estimated to have a 30- to 60- fold higher risk to develop into a deadly esophagus cancer, esophageal adenocarcinoma (Cameron, Ott, and Payne 1985; Drewitz, Sampliner, and Garewal 1997; Kim et al. 1997). A critical review showed that the annual development rate from BE to esophageal adenocarcinoma is 0.5% (Sharma et al. 2004). This relatively rare cancer, only representing 1% of all new cancer cases in the United States, is among the deadliest cancer of all kinds with an estimated death rate greater than 90% in 2016 (Siegel, Miller, and Jemal 2016). The prognosis and treatment option is insufficient, with almost the lowest relative 5-year survival rate of 18.4% in the United States (Howlader et al. 2016). And it is the fifth leading death cancer for males in the age range of 40 to 59 (Howlader et al. 2016).

Two esophageal derived cell lines are chosen for the experiments in this dissertation. (1) Squamous cell culture: EPC2 cell. (2) BE cell line: CP-D cell. The EPC2 cell line is a normal esophageal epithelial cell line transformed with *hTERT* (Harada et al. 2003). While the CP-D cell line is derived from a high-graded dysplasia BE patient and display *CDKN2A* and *TP53* abnormalities (Palanca-Wessels et al. 1998). The CP-D and EPC2 spheroids were mixed together to simulate premalignant condition. Furthermore, these two cell lines have different mRNA expression profiles which can be used to identify the cell types. A specific endogenous gene is needed to discriminate different cell lines. This endogenous

gene is only highly expressed in one particular cell line and can be used to differentiate cell lines by analyzing the gene expression patterns. This part will be discussed in Section 3.3.

3.2 Cell culture

Two cell lines were used in the laser lysis experiments, EPC2 and CP-D. The EPC2, a non-cancerous cell line, was cultured using Gibco keratinocyte serum-free cell growth medium (Invitrogen, Carlsbad, CA, USA), supplemented with human EGF at 2.5 µg/500 mL, BPE (bovine pituitary extract) at 25 mg/500 mL and penicillin–streptomycin solution (Invitrogen) at 100 units/100 µg/mL (Gibco). Dysplastic BE CP-D cells were cultured with the same protocol and buffer as EPC2 cell line. All the cells were cultured at 37°C in a humidified incubator containing 5% CO2 and passaged upon reaching 70-80% confluency. The passaged cells were used for cluster cell formation. Cells were cultured using Gibco keratinocyte serum-free cell growth medium supplemented with human EGF at 2.5 µg/500 mL, BPE (bovine pituitary extract) at 25 mg/500 mL and penicillin-streptomycin solution (Invitrogen) at 100 units/100 µg/mL. The cell density was determined using a Countess® II FL Automated Cell Counter (Life Technologies). The cells were seeded at a density of 150,000 per well of a Costar 24 well plate with ultra-low attachment surface (Corning, Midland, MI) containing 500 µL of differentiation medium (1 part of the media was conditioned by primary human fibroblasts and 50 parts by RPMI with 10% fetal bovine serum). Cells were allowed to cluster for 48 hours at 37°C in a humidified incubator containing 5% CO2.

On the day of experiment, cell clusters were centrifuged at 900 rpm for 3 minutes and re-suspended in 1 mL of XF Base medium (Seahorse medium). A few microliters of

cell culture suspension was dispensed into a Terasaki plate with a goal of obtaining approximately 2 or 3 clusters in each well, and these cells were ready to load.

3.3 Gene validation

Four genes: *rbcL*, *HSP70*, *RPLP1*, and *MUC1* were chosen for single-cell laser lysis RT-qPCR in this research. *RPLP1* was selected as the housekeeping gene for its excellent stabilities and high expression level that has been well documented before (Steg et al. 2006; He et al. 2008; Minner and Poumay 2009; Wang et al. 2012). Also, *RPLP1* could be used as the reference gene to calibrate other genes when multiple gene expression analysis was performed. *rbcL* was spiked in each collection sample before RNA purification as an exogenous gene to minimize systematic error. *HSP70* has already been used to enhance cell resistance in terms of its responses to environmental stresses for years (Li and Werb 1982; Jäättelä et al. 1992; Jäättelä et al. 1998). In this study, *HSP70* was used to validate the different gene expression patterns in cellular stress response between laser lysis and chemical lysis.

The endogenous gene is the key factor to differentiate CP-D and EPC2 cell types. The ideal endogenous gene should have the ability to differentiate specific cell lines from the qPCR result in terms of Ct value. Several genes were validated using a serial dilution approach with CP-D and EPC2 cell lines. A one-step RT-qPCR method was developed to validate these genes, which is described as follows.

The first step was chemically lysing the bulk cells. The RNA lysis buffer was added to bulk cells and the RNA purification was performed using ZR quick RNA MicroPrep Kit (Zymo Research, Irvine, CA) following the instructions provided by the manufacturer. A

total of 50 µL RNA was eluted from a column matrix and quantitated on a Nanodrop 1000 spectrophotometer (Thermo Scientific, Hudson, NH) to determine the total amount of RNA in bulk cells. The RNA was diluted accordingly to achieve a single cell level (20 pg RNA) and prepared for the reverse transcription and quantitative PCR analysis by StepOne PCR system. The total reaction volume was 10 µL, containing 5 µL 2X qPCR buffer (Invitrogen # 11784200), 1 µL of each primer at 4 µM, 0.2 µL EXPRESS One-Step Superscript® qRT-PCR Kit universal (Invitrogen #11781200), 0.1 µL ROX reference dye, 0.7 µL DNA suspension buffer, and 2µL RNA. The RT-qPCR result of different tested genes is shown in Table 1. A total of 5 genes was tested with two technical replicates, the 10 and 100 denoted quantity of cells in terms of 200 and 2000 pg RNA amount. PCR primers for four target genes (*rbcL*, *HSP70*, *RPLP1*, and *MUC1*) used in single cell RT-qPCR were as shown in Table 2.

Table 1. Endogenous Gene Expression between CPD and EPC bulk cells. This Table shows different gene expressions with CP-D and EPC2 cell lines. 100, and 10 indicate 100 and 10 single cells determined by 2000 and 200 pg RNA. From the result of MUC1, there was about a 4-cycle difference between CP-D and EPC2 cells either in the 100 or 10 cells group, specifically around 16-fold change between CP-D and EPC2 cells.

	DCN-4		ITGB6-2		MUC1		MUC16-2		WNT7A-5	
	Ct	STDV	Ct	STDV	Ct	STDV	Ct	STDV	Ct	STDV
CPD 10	26.96	0.16	26.8	0.12	24.98	0.01	25.41	0.31	27.86	0.09
CPD 100	24.42	1.1	23.68	0.3	21.69	0.04	22.46	0.03	25.5	0.06
EPC2 10	29.17	0.52	25.33	0.1	29.32	1.02	25.75	0.01	28.07	0.08
EPC2 100	27.17	2.41	22.24	0.33	26.17	0.87	23.01	0.01	24.66	0.02

Table 2. Genes and Corresponding Primers.

Gene	GeneBank Accession No. and product size (bp)	Primer sequence
RPLP1	NM_213725.1 121 bp	F: 5’-TCACTTCATCCGGCGACTAG-3’ R: 5’-ACTGTCACCTCATCGTCGTG-3’
MUC1	NM_001204296.1 195 bp	F: 5’-CTGGTCTGTGTTCTGGTTGC-3’ R: 5’-CTCATAGGGGCTACGATCGG-3’
HSP70	NM_005345.5 213 bp	F: 5'-CGACCTGAACAAGAGCATCA-3' R: 5'-AAGATCTGCGTCTGCTTGGT-3'
rbcL	CP000435.1 180 bp	F: 5'-CGCTGAATCTTCAACTGGTACCTGGTC-3' R: 5'-GGTCAGAACGTTAGTGATTGAACCCTC-3'

3.4 Results and discussion

The results in Table 1 present the five endogenous genes expression patterns with CP-D and EPC2 cell lines. The CP-D and EPC2 10, 100 denote 10 and 100 single cells. Each qPCR analysis was performed with one biological replicate and two technical replicates. The differences of Ct value between the CP-D and EPC2 cell lines were clearly shown in Table 1. All the other four genes (DCN-4, ITGB6-2, MUC16-2, and WNT7A-5) had Ct differences ranging only from 1 to 3, while *MUC1* had the highest Ct difference (greater than 4) which makes it an excellent candidate to distinguish CP-D from EPC2. Additionally, the Ct differences from CP-D 10 to CP-D 100, and from EPC2 10 to EPC2 100 were 3.3, which perfectly corresponds to a 10-fold change in bulk-cell populations. This also validated the accuracy of the serial dilution in terms of RT-qPCR result. Therefore, *MUC1* was selected due to the high expression level in one particular cell line.

3.5 Conclusion

In summary**,** the gene selection played a very critical role in the whole laser lysis research after the target cell lines were selected. Considering the limited amount of one single cell lysate and low copy numbers of genetic properties, an ideal gene is a necessity to analyze cellular gene expression at the single-cell level. Here, *RPLP1* was selected as the housekeeping gene due to the high expression level in both CP-D and EPC2 cell lines. Additionally, the *RPLP1* can be used to calibrate with other genes when multiple genes are measured at the same time within one single cell. *HSP70* was chosen to validate the cellular stress between the control and heat-shock treated cells. For differentiating mixture-cell clusters, the *MUC1* was selected owing to the distinct Ct value difference between CP-D and EPC2 cell lines. By analyzing the gene expression patterns, the heterogeneity and biological significance can be quantified at the single-cell level.

4. LASER LYSIS CHIP

4.1 Introduction

Microfluidic devices have been developed for a long time with numerous applications (Whitesides 2006), such as chemical screening (Hansen et al. 2002), separation with mass sorting (Ramsey and Ramsey 1997), drug development (Dittrich and Manz 2006), bioanalysis (Sia and Whitesides 2003), and cell-manipulation (Wheeler et al. 2003; Werdich et al. 2004). Different techniques have been developed in order to trap or manipulate cells, including mechanical trapping geometry or micromanipulation (Carlo, Wu, and Lee 2006; Anis, Holl, and Meldrum 2010), hydrodynamic trapping structure (Chen et al. 2015; Chen et al. 2016), dielectrophoretic force (Arnold and Zimmermann 1988; Voldman et al. 2003; Murata et al. 2009), acoustic wave (Meng et al. 2011), and optical force (Huang et al. 2013; Huang et al. 2014; Burghammer et al. 2015). Among all techniques, a mechanical trapping structure is advantageous for laser lysis chip fabrication. Firstly, it does not require any specialized on-chip fabrication such as electrodes for dielectrophoretic force. Secondly, it has a simple trapping design that reduces greatly the labor and cost of chip fabrication and operation. The design and fabrication of the laser lysis chip are discussed as follows.

4.2 Laser lysis chip design

There are three major goals in laser lysis chip design: (1) Capable of capturing cell cluster of size 40-100 μm diameter, practical for analyzing clinical biopsies. (2) Capable of retaining the cluster during the cell loading, perfusion and lysis. (3) Minimize contamination during the experimental process. Based on these requirements, the cell

cluster trapping design “cage” was composed of several posts used to trap flow-through cell clusters while the media flowed through the gap spaces between posts (Figure 3c). The post width was 42 μm and the gap distance in between was 18 μm (Figure 3b), which allowed small single cell to bypass cage yet most large cell clusters (size between 40-100 μm) stay. Namely, the gap was small enough to retain clusters during the lysis process yet large enough for media to bypass. For the microchannel design, the dimension of microchannel was 500 μm in width and 100 μm in depth which could fit the sizes of most cell clusters and clinical tissues (Figure 3c). In order to prevent contamination, an oil channel was introduced on the side. Details of cross-contamination are discussed later. The cage design was made by AutoCAD program (Autodesk Inc, San Rapheal, CA) then transported to a bright-field photomask for a photolithography process on a silicon wafer as the master mold. At last, the laser lysis chip was fabricated by using soft lithography techniques with PDMS material. Details are covered in the next section.

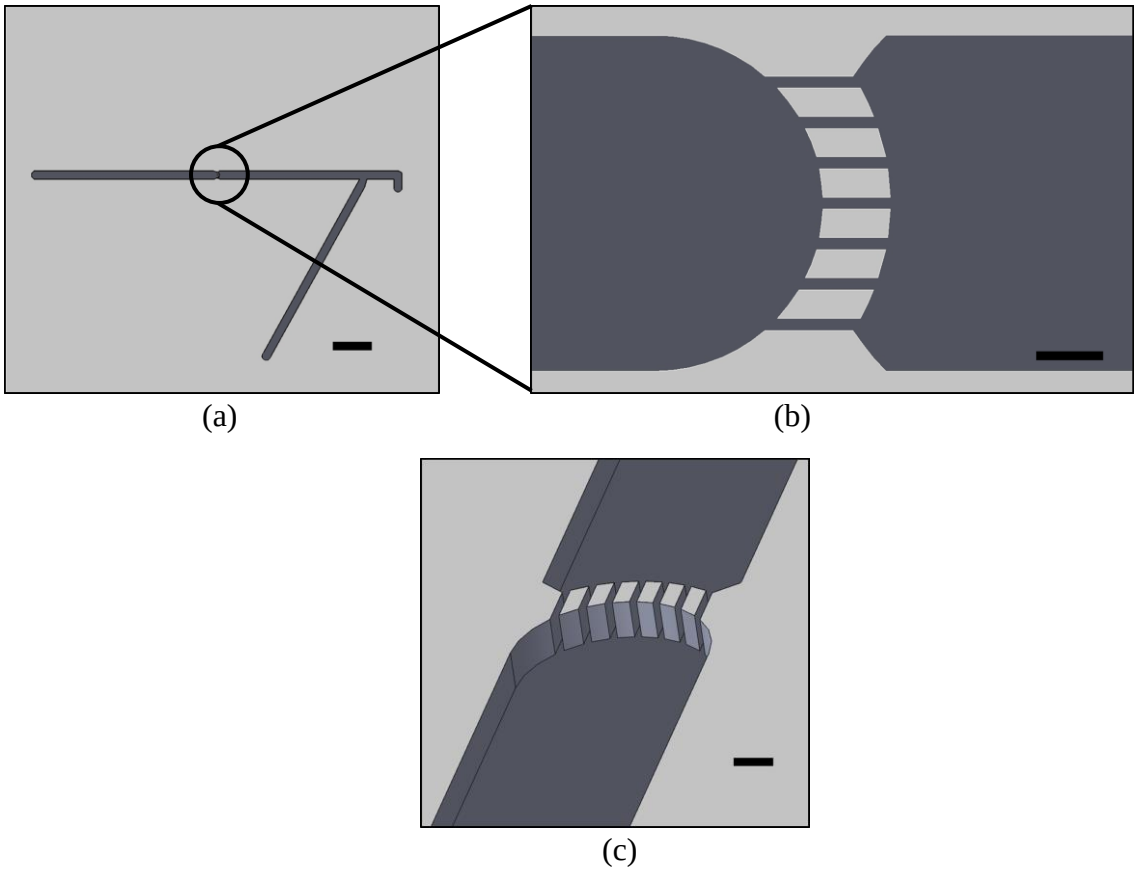

Figure 3. Laser Lysis Chip Design. (a) Laser lysis chip layout. Scale bar: 2 mm. (b) Cage design. Scale bar: 100 μm. (c) Enlarged schematic of cage. Scale bar: 100 μm.

4.3 Fabrication

Fabrication of the laser lysis chip utilized soft lithography technology. The concept of soft lithography has been developed since Bell Labs designed the first micromolding device in 1974 (Aumiller et al. 1974). Soft lithography techniques can be used to fabricate microfluidic devices through molding, stamping, and embossing (Aumiller et al. 1974; David J. Beebe, Glennys A. Mensing, and Walker 2002). Several semiconductor technologies and equipment are applied in the laser lysis chip fabrication process. The

fabrication processes include the master wafer fabrication, wafer dicing, PDMS chip molding process, and chip bolding. Several critical factors need to be considered during laser lysis chip fabrication: firstly, the depth of the microchannel. The dimension of microchannel was critical since the high-aspect-ratio structure increases fabrication difficulties. Secondly, the cage design was also affected by the high-aspect-ratio patterning for its three-dimension structure. The etching effect was server for post fabrication, since the gap between each post determined different sizes cell trapping. Thirdly, the alignment process for via-channel aligned to the microchannel inlet and outlet end.

4.3.1 Material

PDMS was used to fabricate laser lysis chip. PDMS has been used as a material for microfluidics since it has several advantages such as being easy to fabricate and low-cost. PDMS is especially suitable for biological studies due to the biocompatibility and transparency, also it easily bonds with other substrates such as glass (Sia and Whitesides 2003). The highly transparent glass is a perfect substrate for optical imaging. In order to observe and perform lysis on single cells at high magnification, the glass thickness was crucial for high magnification imaging. A 25 mm × 25 mm micro cover glass with thickness of 200 μm (VWR Scientific Inc., West Chester, PA) was used as a substrate. Silicon wafer was used as master substrate for high-aspect-ratio patterning with photolithography techniques.

4.3.2 Fabrication process

4.3.2.1 Master wafer

The laser lysis chip fabrication consisted of two steps: first step was master wafer fabrication, second step was chip molding. The fabrication process of laser lysis chip is illustrated in Figure 4. The master fabrication started with a 4-inch silicon wafer of 500 μm. The silicon wafer was placed in ultrasonic isopropyl alcohol for 10 min, rinsed thoroughly with DI water (Figure 4a). The wafer was placed on a 160°C hot plate for 5 min. The wafer was spin-coated with SU-8 3025 negative photoresist (MicroChem Corp., Newton, MA) at 3800 rpm and softbaked at 65°C for 1 min then 95°C for 5 min, with the ramping temperature controlled at a rate of 1°C/min (Figure 4b). The coated wafer was then exposed at 150mJ/cm^2 with PL360-LP filter (Omega Optical Inc., BRATTLEBORO, VT) (Figure 4c), followed by performing the post-exposure-bake with the same temperature setting as softbake then developing by SU8 developer (MicroChem Corp., Newton, MA), and rinsing with isopropyl alcohol to inspect the pattern. Finally, the wafer was hardbaked with a ramp up rate of 1°C/min at 150°C for 40 min. The wafer was dry etched by Advance Silicon Etch (Surface Technology Systems, Newport, UK), an inductively coupled plasma reactive ion etching system to perform vertical high-aspect-ratio etching (Figure 4d). After DRIE process was done, the wafer was diced into six dies with a Disco dicing saw (Disco Hi-Tec Inc., Santa Clara, CA).

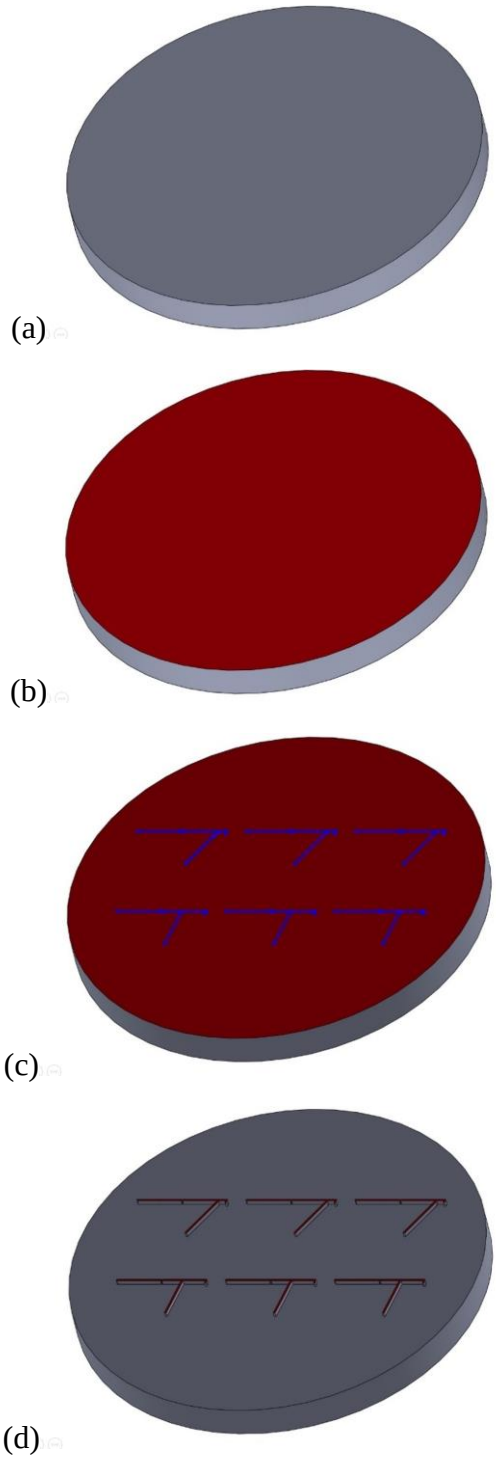

Figure 4. Master Wafer Fabrication Process. (a) Silicon wafer. (b) SU8 3025 spin-coat. (c) Microchannel patterning. (d) DRIE process.

4.3.2.2 Laser lysis chip one-step molding

The second step was laser lysis chip molding. A novel approach for PDMS chip molding was developed at this stage. Compared with traditional PDMS microfluidic device fabrication which requires punching microchannels after PDMS is cured, a one-step molding was established that combines PDMS curing process and developing inlet and outlet channels at the same time. The one-step molding contains three parts: the molding base, supporting layer, and the lid. The laser lysis chip was adhered on the molding base then placed on the supporting layer for PDMS molding (Figure 5a). PDMS was made from a mixture of 1:10 curing agent to base polymer (Silicone Elastomer 184, Dow Corning Corp., Midland, MI), then poured into the chip mold. The final step was covered the mold with lid. The lid was designed with three fine alignment pin holes that perfectly match the microchannels on the chip. After covering up the lid, three 1/64" pins were inserted to develop the inlet and outlet channels while the PDMS was cured (Figure 5b). The chip mold was left at 65°C for 1 day then dissembled the one-step molding to peel off the cured PDMS laser lysis chip. A 25 mm × 25 mm micro cover glass was bonded with the PDMS chip with 10W RF-power plasma treatment (Harrick Plasma, Ithaca, NY) (Figure 5c).

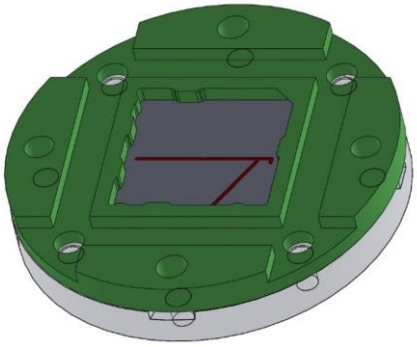

(a)

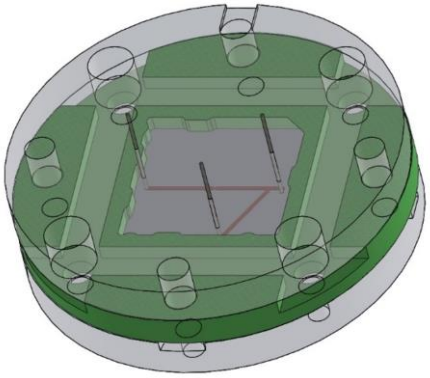

(b)

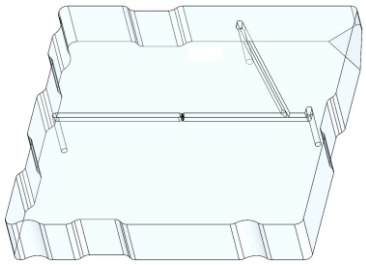

(c)

Figure 5. Laser Lysis Chip Molding by Using One-step Molding Process. (a) Chip assembling to PDMS mold. (b) Alignment lid for inlet and outlet channels. (c) Chip bonding with cover glass. (Not to scale)

4.3.2.3 One-step fluid interface

Conventional microfluidic devices use nanoports or peek tubes with adapters for fluidic connection. However, it is usually labor-intensive and low efficiency to do so. Thus, another approach being made is a one-step fluid interface. One-step fluid interface is an integration development for fluidic connection which reduces the labor for tubing connection. The design of one-step fluid interface was followed by the location of pin holes on one-step molding lid. The connection process was straightforward, aligned three notches on laser lysis chip to three posts on the interface. Then the inlet, outlet of the laser lysis chip would be connected to the fluidic interface (Figure 6). The laser lysis chip was then secured by a sandwich structure as shown in Figure 11.

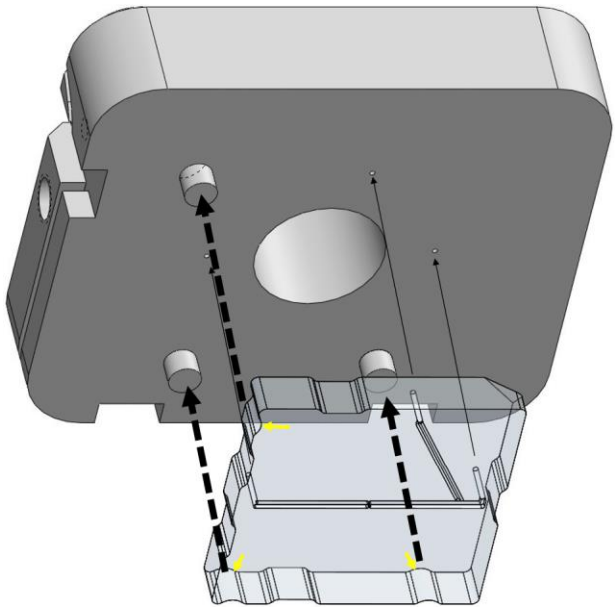

Figure 6. One-step Fluid Interface. Three posts (dashed arrows) on one-step fluid interface align perfectly with three notches (yellow arrows) on laser lysis chip. Next, all the inlet, outlet are aligned to the fluid interface.

4.4 Results and discussion

The laser lysis chip design has been revised through a couple of different versions to reach the final version as shown in Figure 3. Figure 7 shows the previous version of the cage design. Compared with these two designs, the oil channel was moved away from the center cage region in order to prevent the oil from back flushing to the cage area which caused cross-contamination. The oil channel input in the previous design was too close to the cage area to contaminate the lysates of single cells. This issue has been solved after moving the oil channel downstream.

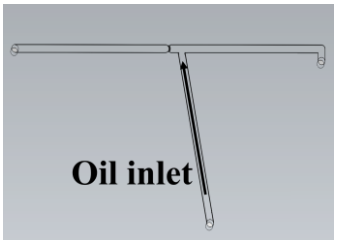

Figure 7. Previous Laser Lysis Chip Design.

There were other problems that showed up in fabrication process of the laser lysis chip: the first was the high-aspect-ratio of the microchannel and the cage structure due to the critical dimension. The other was the alignment of inlet and out channels, which was solved by using the one-step molding process. The one-step molding simplified the inlet, outlet channels development and reduced molding steps which may minimize contamination. Another approach is one-step fluid interface which increases efficiency and requires less labor.

The critical structure of the microchannel depth and cage was fabricated using the DRIE equipment. However, the cage structure was under-etched due to the critical

dimension of the cage design. Figure 8 shows the cross-section view at the cage in the PDMS laser lysis chip. The result clearly shows that there was a height difference between the posts and the microchannel. This is due to the aspect ratio dependent etching (ARDE) effect in deep silicon etching processes (Lai, Johnson, and Westerman 2006). The ARDE effect is a very common phenomenon especially in many high-aspect-ratio 3D structures. The etch rate is limited by the trench width and the aspect ratio. Figure 9 presents the cage schematic and a comparison between the ideal etching and ARDE effect. Figure 10 shows how the ARDE effect appears on the laser lysis wafer at the cage area. This issue, however, did not interfere with the laser lysis process nor the cell loading or trapping processes. Furthermore, it brought advantages to this research, which will be described in a later chapter.

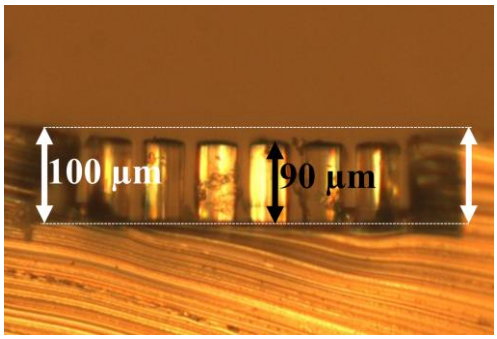

Figure 8. Cross-section View at the Cage on the PDMS Chip.

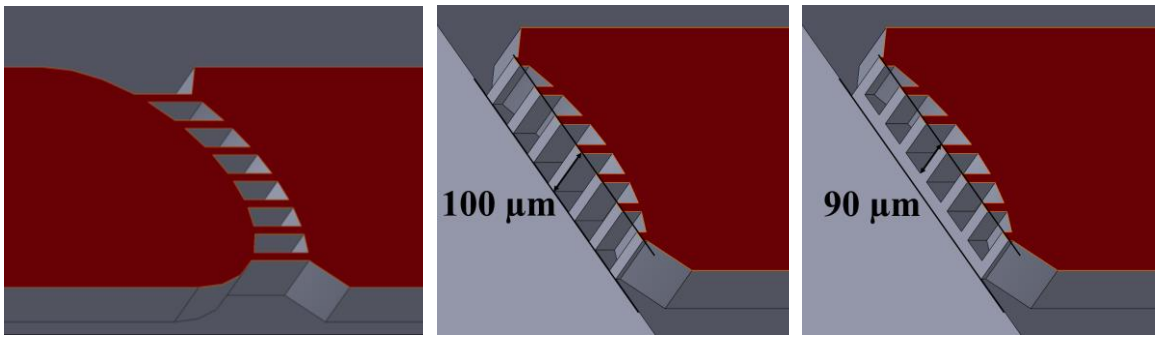

(a) (b) (c)

Figure 9. Schematic of the Cage Structure. (a) Laser lysis wafer after DRIE etching. (b) The cross-section view of the cage. (c) The cross-section view with ARDE effect.

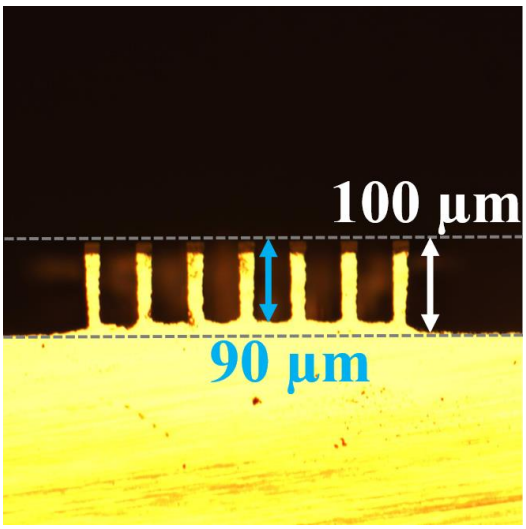

Figure 10. The ARDE Effect on the Laser Lysis Wafer.

4.5 Conclusion

Several important factors are discussed in the design and fabrication part: firstly, the size of cell clusters are critical when designing the cage dimension. Secondly, one-step molding process not only solves inlet, outlet channels development issue but also minimizes possibility of contamination. Thirdly, one-step fluid interface provides an efficient and robust method for fluidic connection. At last, the high-aspect-ratio design of the cage is causing the aspect ratio dependent etching effect. The etch rate is delayed by narrowing the trench width and increasing the aspect ratio. However, this effect did not bring any disadvantages to this research, which will be discussed at the cell-lysis chapter.

5. LASER LYSIS SYSTEM CHARACTERIZATION

5.1 Introduction

The laser lysis system includes the syringe pump, connection tubing, chip loading platform, and laser lysis chip. The laser lysis chip development is discussed in Chapter 4. The chip loading platform was composed by the tubing system which introduced Seahorse medium and oil into chip, then delivered lysates to outlet (Figure 11). Since our goals are lysing cells, collecting and analyzing the released contents from cells. The system needs to be sterilized and optimized to a level in order to mitigate any contamination or RNA lost. In this chapter, the optimization of how to increase RNA retrieval rate will be discussed. We will also compare the laser lysis to the traditional chemical lysis in terms of the mRNA retrieval efficiency. Additionally, the validation of induced cellular stress caused by the laser lysis will be discovered.

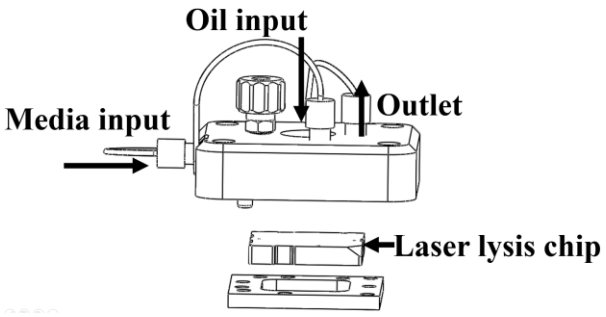

Figure 11. Chip Loading Platform.

5.2 Collection optimization

5.2.1 Sterilization

The laser lysis system has multiple parts, including the tubing, chip loading platform, and laser lysis chip. The downstream RT-qPCR analysis also requires using different biotechnology equipment; therefore, it is very important to sterilize the whole system and equipment. In order to prevent contamination during RNA collection, all Eppendorf tubes and pipette tips were autoclaved before experiment. The polytetrafluoroethylene (PTFE) tubing with 1 mm OD x 0.5 mm ID (DuPont, Wilmington, DE) was selected for the system connection tubing due to its non-fouling surface and inert properties with most chemicals. The system (including loading platform and lysis chip) was pre-cleaned with 1 mL of RNaseZap (Ambion®) to decontaminate all the surface RNA and rinsed with 5 mL of DNase/RNase-free water (Invitrogen™).

5.2.2 PEG treatment

The non-fouling characteristic of the PTFE tubing can minimize the RNA adhesion. However, the PDMS microchannel is known to absorb biomolecules including RNA. To mitigate the absorption of RNA, polyethylene glycol (PEG) coating was applied on the surface. PEG has widely used to heighten biocompatibility and could be covalently bonded to surfaces to reduce RNA/protein binding (Wolf et al. 2004; Charles et al. 2009; Convert et al. 2012). The system was washed with 0.1% w/v PEG 5000 (Laysan Bio, Arab, AL) in 98% ethanol, 3 mL of DI water, and finally sterilized with RNaseZap and RNase-free water.

An experiment was designed to test the ability of PEG surface treatment to minimize the RNA adhesion in the laser lysis system. Two laser lysis chips were prepared

for the experiment: one with PEG coating and the other without treatment as a control. At the beginning of the experiment, the pure media was injected into the chip as a control, followed by the *rbcL* media and collected the flow-through in Eppendorf tubes for two-step RT-qPCR analysis as discussed before. The *rbcL* mRNA levels were measured to compare the PEG coated microchannel with the non-treatment device.

5.2.3 Diffusion contamination

PEG coating can prevent RNA absorption and reduce RNA contamination on the tubing interface. However, another concern is the diffusion contamination between the lysates. The lysates contain cell released contents, which are not uniformly distributed (Figure 12a). Therefore, the diffusion contamination can be an issue while collecting a sequence of lysates from the target cells. One way to solve this issue is to wash the tube in between collection; however, it is time consuming and not effective. An alternative approach is to encapsulate the cell lysate with mineral oil right after lysis (Figure 12b), which can create a physical barrier in between the lysates of different cells (Figure 12c).

We performed an experiment to test the oil separation method by analyzing the mRNA levels. Two syringes, one with the mineral oil and the other with the pure media/*rbcL*-spiked media, were injected into the laser lysis chip simultaneously then collected in the Eppendorf tubes. First, the oil and pure media were introduced into the device at a stable rate (5:50 µL/min). Next, switched the pure media to *rbcL*-spiked media for mRNA collection. In the end, replaced the *rbcL*-spiked media by pure media. Figure 12c shows the media progression flow being separated by the oil. These tubes were centrifuged down to separate oil and media, and then the oil was discarded by a pipette.

The media was then analyzed by the two-step RT-qPCR analysis to measure the *rbcL* mRNA levels.

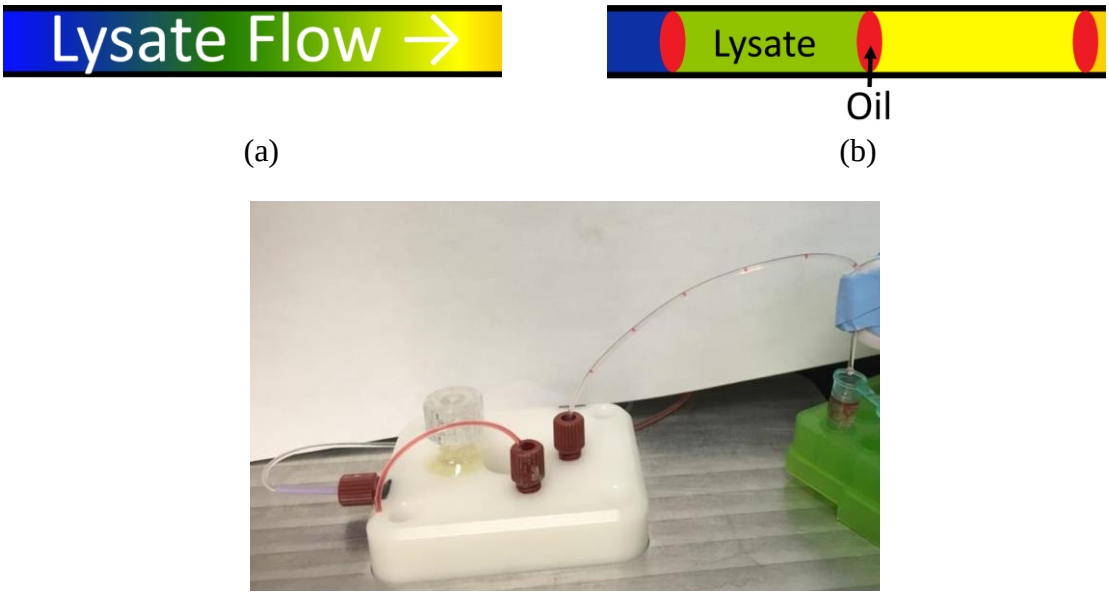

Figure 12. Schematic of Diffusion Contamination. (a) Diffusion contamination in the lysates. (b) Separation lysate by introducing oil. (c) Oil separating the lysate.

5.2.4 Tubing characterization

The amount of collection volume, which is strongly affected by the volume of laser lysis chip, inlet and outlet tubing, is another critical factor in the laser lysis collection. If the collection volume is insufficient, the mRNA within one single cell will be separately collected. On the other hand, over collecting will result in cross-contamination of the mRNA from the next single cell. In particular, this factor will greatly affect the RNA

analysis result in the mixture-cell clusters experiment. This result was due to the laser lysing the single cells with different cell lines consecutively. Therefore, a tubing characterization experiment was designed to determine the correct amount for each collection.

We used the same experiment setup in the diffusion contamination. The amount of each collection was 100 µL, with 50 µL oil and 50 µL media. After centrifuging, the oil was discarded and the media went through the two-step RT-qPCR process for analysis.

5.3 Effciency comparison – laser lysis and chemical lysis

The chemical lysis (lysis buffer) method has been used on cell lysis and developed for years (Irimia, Tompkins, and Toner 2004; Brown and Audet 2008). Several studies have developed different devices like microarrays or microwells to perform single-cell chemical lysis (Sasuga et al. 2008; Zare and Kim 2010; White et al. 2011; Jen, Hsiao, and Maslov 2012). However, no comparison has been made between these two methods in terms of the mRNA retrieval efficiency. In this section, an experiment was designed to compare the efficiency and specialty between the laser lysis and the tradition chemical lysis at the single-cell level. Chemical lysis can be performed by utilizing the serial dilution method to isolate single cells into a 72 multi-well Terasaki plate (Sigma-Aldrich, St. Louis, MO). For laser lysis, a microwells device called PDMS Terasaki chip (PT chip) was designed and fabricated for single-cell lysis.

The PT chip was designed and developed for performing single cells laser lysis. Figure 13 shows the PT chip fabrication process. We used the Benchman MX CNC machine (Light Machines, Manchester, NH) to fabricate the master mold for PDMS molding. Next,

the cured PDMS chip was bonded with a 200 μm thick cover glass. The CP-D single cells were dispensed into each well by the serial dilution method. We used two-photon laser to lyse the single cell in each well. The media was collected for the two-step RT-qPCR analysis.

For chemical lysis, the CP-D single cells were dispensed into the terasaki plate with the concentration of one single cell per well. The lysis buffer was added to each well for 10 min then collected for the two-step RT-qPCR analysis.

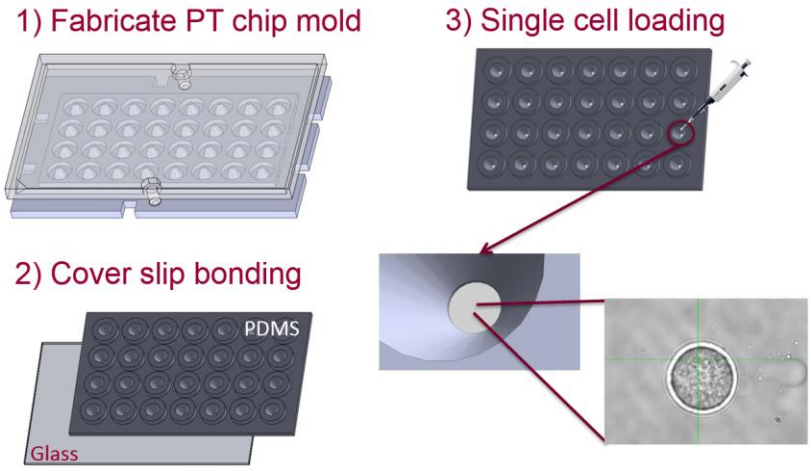

Figure 13. PDMS Terasaki Chip Fabrication.

5.4 Cellular stress validation

A major concern of the single cell laser lysis on 3D cell clusters is the cellular stress induced by the laser. Since the single cell mRNA levels can change due to cellular stress or RNA degradation, we believed that the laser lysis processing time was too short to

induce any stress on the single cells. It is necessary to conduct an experiment to validate the cellular stress caused by laser lysis.

We conducted an experiment by lysing single cells from two groups of cell clusters: one was CP-D clusters as a control and the other was heat shock treated CP-D clusters. The control group was directly loaded into the laser lysis chip after the cell culturing study as described before. Meanwhile, the heat shock treated cell clusters were placed on a 42°C heat block for 10 min then loaded into the laser lysis chip to perform lysis. Both groups were lysed by two-photon laser and the lysates were analyzed by the two-step RT-qPCR method.

5.5 Results and disscusion

5.5.1 PEG treatment

The comparison result in Figure 14 shows that the relative *rbcL* mRNA levels collected from the PEG treated and non-treated devices. The pure media was perfused into the chip as a control in the first tube, followed by injecting the *rbcL*-spiked media. In the end, the input was changed back to the pure media for comparison. The result clearly shows that the PEG treatment device resulted in significantly higher levels of *rbcL* mRNA during the whole collection when the *rbcL* media passed through the microchannel. It could be concluded that the PEG coated PDMS microchannel can minimize the RNA absorption.

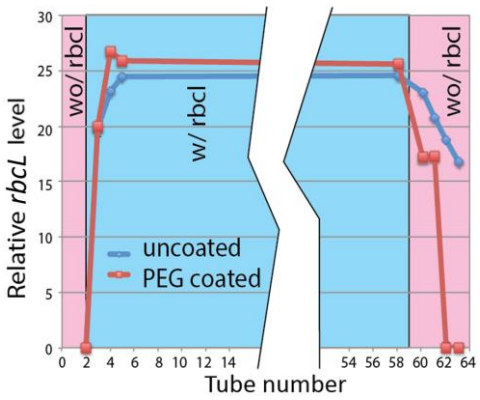

Figure 14. Comparison of Relative *rbcL* Level with PEG Treatment.

5.5.2 Diffusion contamination

Figure 15 shows the relative *rbcL* level with oil separation method. Again, we used the same experiment setup with perfusing the pure media at the first tube as a control as well as at the end of collection. This time, we inspected the transition between the pure and *rbcL*-spiked media. The result shows that the transition was very distinct between the pure

and *rbcL* media. The drastic increase and decrease of the *rbcL* level in the beginning and tube 13 strongly demonstrated that the mineral oil introduction helps to reduce the diffusion contamination.

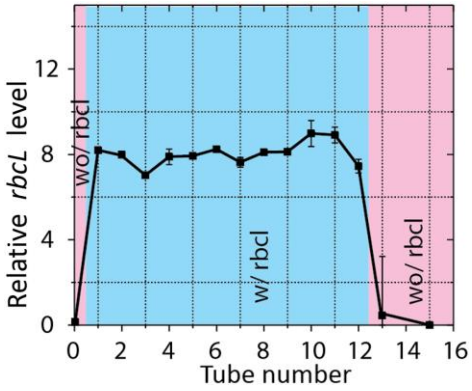

Figure 15. Relative *rbcL* Level with Oil Separation.

5.5.3 Tubing characterization

The RNA collection efficiency has increased after the characterization of PEG treatment and oil introduction; however, the collection amount of media for each tube or for each lysed single cell is still crucial considering lysing single cells with different cell lines. In this experiment, the total volume of the laser lysis system was measured as 242 µL, the input and output tubing was 242 µL, and the microfluidic channel was less than 1 µL. The collection amount in this experiment was 100 µL for each tube contained 50 µL oil and 50 µL media. Figure 16 shows the result of tubing characterization. The collection sequence followed the same experiment setup as before: collected pure media in the first tube, and then started to collect *rbcL*-spiked media at tube 2, finally switched back to pure media at

tube 11. The *rbcL* mRNA level started to increase at tube 6 with the result that the collection amount from tube 1 to 5 surpassed the total volume of laser lysis system. Considering the media volume in each tube was only 50 µL, the *rbcL*-spiked media would flow through the outlet Eppendorf tube at tube 6. The result perfectly shows that how the system volume affects the collection volume. For the ending collection, the system was flushed with pure media after tube 10 which resulted in the mRNA level decreased at tube 11.

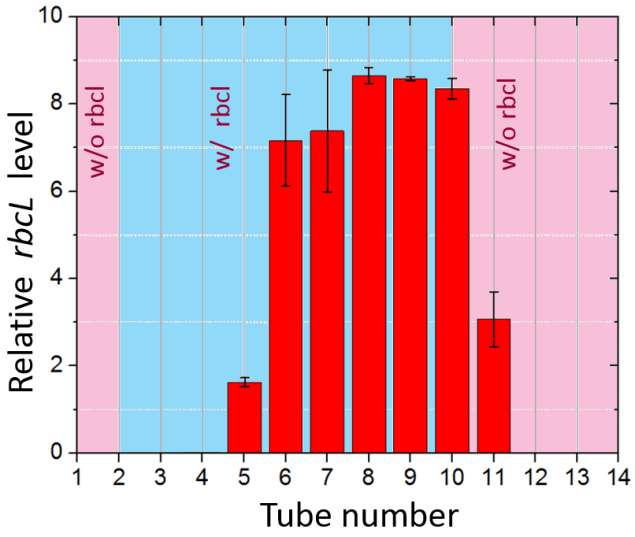

Figure 16. Relative *rbcL* Level for Tubing Characterization.

5.5.4 Efficiency comparison - laser lysis and chemical lysis

Two different lysis methods were applied on CP-D single-cell lysis. In order to compare the gene expressions across different conditions and analytical methods, the expression measurement needs to be normalized against a reference gene (Heid et al. 1996). In this study, the lysate collection was analyzed with *RPLP1* and *rbcL* mRNA, which represents as the housekeeping and exogenous gene respectively. The *RPLP1* mRNA acted as the

lysis indicator due to the high expression level in CP-D cell line, and the *rbcL* mRNA acted as a reference gene with the result that it had constant copy number in all cells. The result was analyzed by ddCt method (Livak and Schmittgen 2001; Pfaffl 2001), which was calculated by the Ct value of the target gene against to the reference gene and then normalized to the calibrator. We selected *RPLP1* as the target gene, *rbcL* as the reference gene, and positive control (Four CP-D cells) as the calibrator. By using the ddCt method, the raw data of the chemical lysis and laser lysis could transform into Ct differences for analysis. The ddCt results and mRNA fold change, which was calculated by 2^{-ddCt} (Livak and Schmittgen 2001; Pfaffl 2001), are plotted in box chart and shown in Figure 17. Note that the boxes represent the interquartile range (IQR) between first and third quartiles. The line and dot inside represent the median and mean, respectively. Whiskers denote the lowest and highest values within 1.5 × IQR from the first and third quartiles, respectively. The result shows that the laser lysis had better *RPLP1* retrieval rate for it had smaller ddCt value than chemical lysis. For the reason that the smaller the ddCt value, the higher mRNA gene expression. This indicates that the laser lysis is at least 2-fold better than the chemical lysis in terms of lysis efficiency. Additionally, the wide whiskers range of the chemical lysis also revealed that the reproducibility and specificity is relatively low compared to laser lysis.

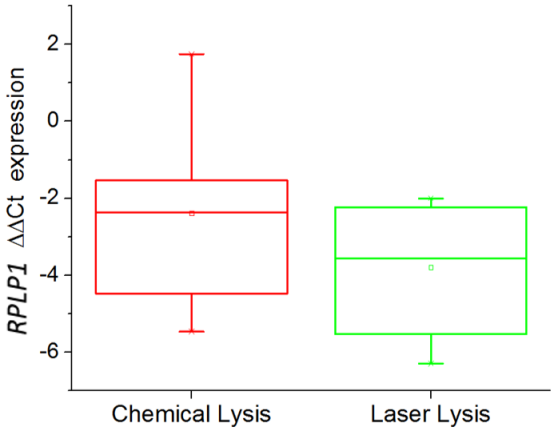

Figure 17. Comparison of *RPLP1* mRNA ddCt Expression between Chemical Lysis and Laser Lysis.

5.5.5 Cellular stress validation

In this study we performed the single-cell laser lysis on two groups of CP-D clusters: one with heat shock treated and the other without treatment as a control. The objective of this experiment is to inspect whether the laser lysis method induces cellular stress on non-treated CPD clusters during lysis process and to quantify the cellular stress level with the heat shock treated CPD clusters.

In order to measure the stress expression levels, the *HSP70* gene was analyzed. The relative gene expression levels were acquired by the ddCt method (Livak and Schmittgen 2001; Pfaffl 2001). In particular, *HSP70* was chosen as the target gene and *RPLP1* as the reference gene. Figure 18 shows the comparison of *HSP70* mRNA expression levels between the heat shock treated group and non-treated in box plot. The difference of *HSP70* ddCt expression levels from the result is very distinct. The HSP70 mRNA was highly

expressed in the heat treated group than the normal group. In other words, the cellular stress induced by the laser was way smaller than the heat treatment. Additionally, Figure 19 shows that there was no significant difference between the laser and chemical lysis. This result indicates that there was no such correlation between the laser and the cellular stress, which was more likely being induced by the cell preparation process or other factors.

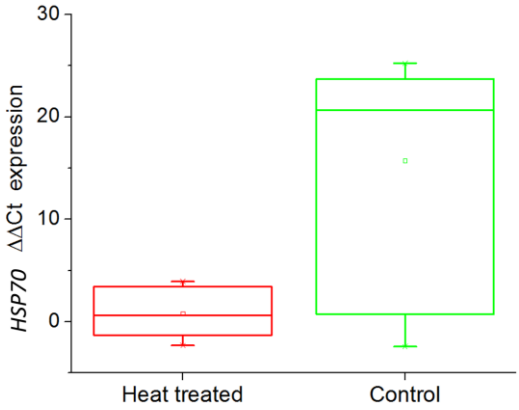

Figure 18. Comparison of *HSP70* mRNA ddCt Expression between Heat Shock Treated and Non-treated Group.

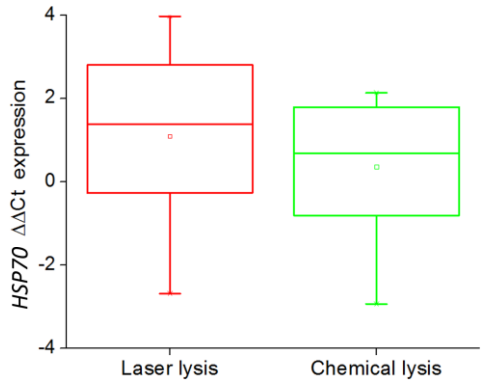

Figure 19. Comparison of *HSP70* mRNA ddCt Expression between Laser and Chemical Lysis.

5.6 Conclusion

In summary, the laser lysis system was optimized by different methods to increase the RNA collection efficiency as well as validate the lysis efficiency and cellular stress. The PEG coating and oil introduction method increased the collection efficiency by reducing RNA absorption and contamination in the laser lysis system. Furthermore, the tubing characterization prevented cross-contamination by collecting the accurate lysate amount, particularly when lysing single cells from mixture-cell clusters. The efficiency characterization between the laser and chemical lysis showed that both methods were capable of lysing the single cells whereas the laser lysis generated highly reproducible and specific results. Although there was concern about the laser-induced cellular stress, based on our results, it could be neglected for the insignificant *HSP70* mRNA expression level.

6. SINGLE CELL RT-qPCR ANALYSIS ON CP-D CELL CLUSTERS

6.1 Introduction

The stochastic gene expression at the single-cell level in an isogenic population is already a well-known phenomenon (Kelly and Rahn 1932; Maloney and Rotman 1973; Siegele and Hu 1997; Lidstrom and Meldrum 2003; Becskei, Kaufmann, and van Oudenaarden 2005; Kuang, Biran, and Walt 2004; Colman-Lerner et al. 2005; Pedraza and Oudenaarden 2005; Rosenfeld et al. 2005; Strovas et al. 2007; Strovas and Lidstrom 2009). The variation of cell-to-cell gene expression comes from the noise of transcriptional regulation, genetic factors, and intrinsic fluctuation (Banerjee et al. 2004; Colman-Lerner et al. 2005; Pedraza and Oudenaarden 2005; Rosenfeld et al. 2005; Newman et al. 2006; Strovas et al. 2007). These variances make single-cell studies much more complicated to analyze. It is more difficult when the study is about cell clusters owning to the complexity of cell-to-cell interaction inside the cell clusters. A number of devices and methods have been developed to study single-cell characteristics (Carlo, Wu, and Lee 2006; Chung, Kim, and Yoon 2011; Jen, Hsiao, and Maslov 2012; Stumpf et al. 2015; Chen et al. 2016b; Ungai-Salánki et al. 2016). These studies were generally focused on single cells separated from bulk-cell populations, thus they were detecting the heterogeneity between each individual cell, not cell-to-cell difference on a tissue-like cell cluster. In this study, we performed single-cell analysis on 3D CP-D cell clusters by using two-photon laser to lyse individual single cell consecutively. Moreover, the lysates were collected and analyzed by the two-step RT-qPCR method which can detect gene expression patterns at the single-cell level. The RNA expressions from the single cells could be traced back to their original locations on the clusters which may use to construct a 3D spatial mapping of gene expressions.

6.2 Experiment

6.2.1 Experiement preparation

Before cell loading, the laser lysis system was sterilized and treated with PEG coating (Chaper 5). The CP-D cell clusters were loaded into the laser lysis chip after cell culturing process (Chapter 3). In order to control the numbers of cell clusters that being loaded into the laser lysis chip; one or two cell clusters were picked from Terasaki plate by a pipette. The selected cell clusters were loaded into the chip via a microchannel inlet by the pipette tip (Figure 20), then the laser lysis chip was assembled with the chip holder. The chip holder consists of a tubing system which introduces Seahorse medium and oil into the chip, and then delivers the lysates to the outlet (Figure 21). The media and oil was introduced by a syringe pump (Harvard Apparatus, Holliston, MA) at a stable flow rate (30:1.6 μL/min) to wash away background signal during lysis process. Figure 21 illustrates the laser lysis chip working platform. Figure 22 shows the trapping results of CP-D and EPC2 cell clusters with different sizes and cluster formations. The results demonstrate that the CP-D cell clusters were easily trapped in a space between the posts and the cover glass (Figure 22b), which was caused by the aspect ratio dependent etching effect (Chapter 4). This effect actually brought advantages both in trapping and lysing processes. In other words, the cells that are trapped in the space are easier to identify and lyse.

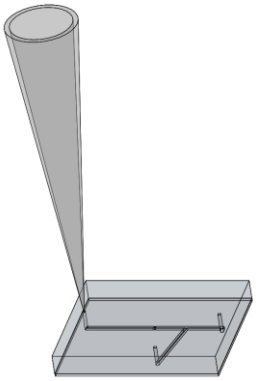

Figure 20. Schematic of Cell Loading.

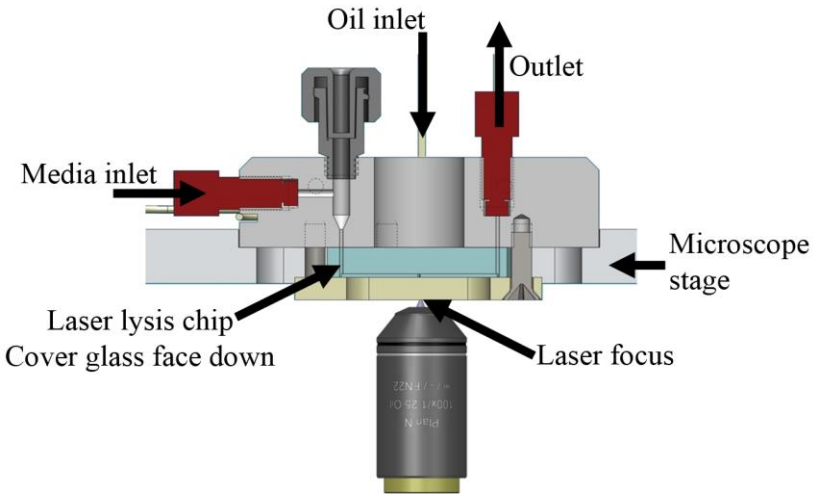

Figure 21. Laser Lysis Working Platform.

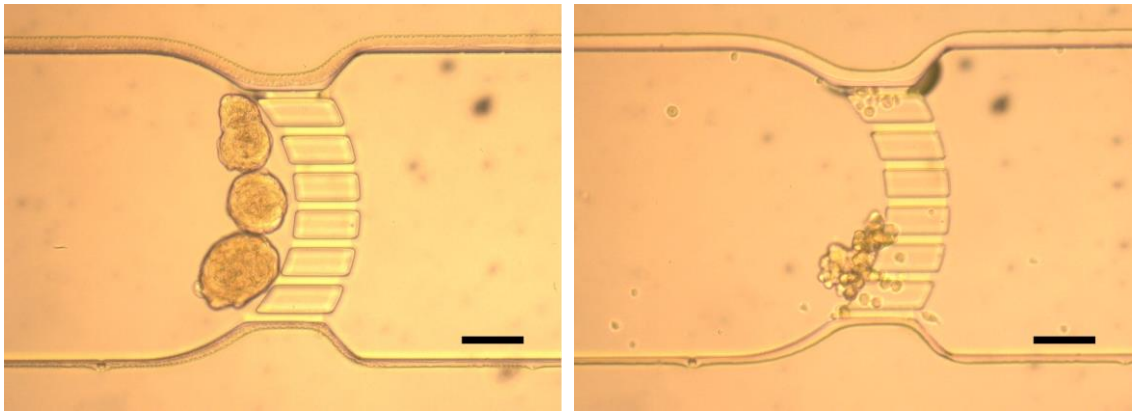

(a) (b)

Figure 22. 3D Cell Clusters Trapping. Scale bar: 100 μm. (a) EPC2 cell clusters trapping in cage. (b) CP-D cell clusters trapping in cage.

6.2.2 Laser lysis

First, CP-D cell clusters were loaded into the lysis chip and stabilized with media flow. Later, the laser lysed on one CP-D single cell with a slow flow rate (media:oil=10:1.6 µL/min) to ensure all the contents released from the cell would be collected in the Eppendorf tube. After the single cell was fully lysed, the cell clusters were washed with a stable media rate of 30 µL/min to clean the background signal thoroughly. In the meantime, three 200 µL Eppendorf tubes were collected from the outlet for each lysed CP-D single cell. The first tube contained all the released contents from the target cell, the second and third tubes had only Seahorse medium. Next, the same procedure was followed to lyse another CP-D single cell for three tubes collection. At last, the collection was analyzed by the two-step RT-qPCR method with *rbcL* and *RPLP1* mRNA. Figure 23 presents the CP-D cell clusters lysis progression. The results show the target CP-D cell was fully lysed during the process and the adjoining cell remained intact after lysis (Figure 23b).

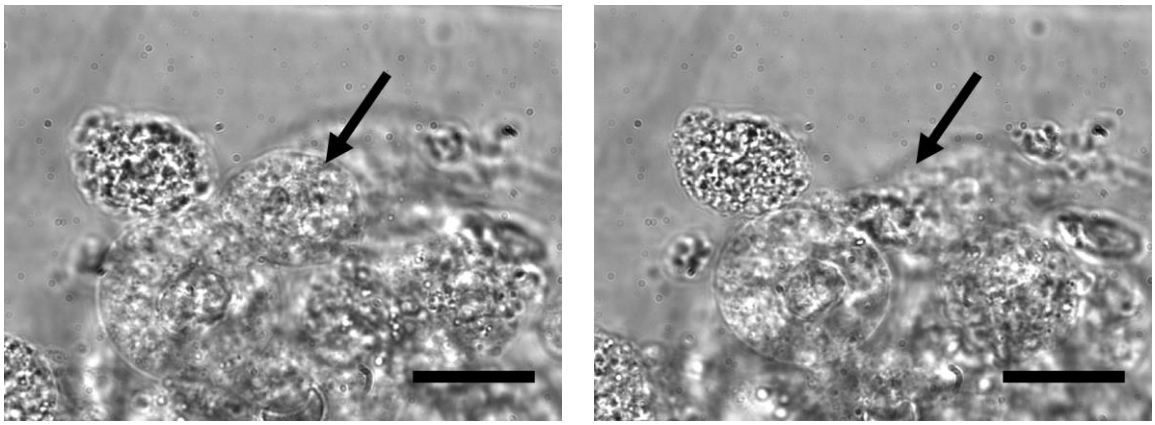

(a) (b)

Figure 23. CP-D Cell Cluster Lysis Process. Scale bar: 20 µm. (a) Target cell before lysis. (b) After lysis.

6.2.3 Two-step RT-qPCR method

Before RNA isolation, each sample was spiked with 1 µL *ribulose-bisphosphate carboxylase (rbcL)* mRNA to validate qPCR process efficiency. A ZR quick RNA MicroPrep Kit (Zymo Research, Irvine, CA) was used to extract the RNA from lysate, and the total RNA was eluted into a final volume of 5.25 µL in Eppendorf microtubes. A SuperScript® VILO™ cDNA Synthesis Kit (Invitrogen # 11754050, Carlsbad, CA) was used to synthesize cDNA. To increase the relative concentration of single-cell mRNA for cDNA synthesis preparation, the total reaction volume was decreased to 7.5 µL, which contained 0.75 µL 10X SuperScript® III Enzyme Blend, 1.5 µL 5X VILO™ Reaction Mix, and 5.25 µL of eluted RNA. After cDNA synthesis, then the template was ready for the qPCR step. The primers for RT-qPCR were designed using Primer-BLAST (http://www.ncbi.nlm.nih.gov/tools/primer-blast/index.cgi?LINK_LOC=BlastHome). To differentiate the PCR products from primer dimers, the primers were selected to generate amplicons with sizes around 170 to 220 bp. The qPCR was performed using Express SYBR GreenER qPCR SuperMix kits (Invitrogen, Carlsbad, CA) on an ABI StepOnePlus real-time PCR system (Applied Biosystems, Foster, CA). The temperature for qPCR is 5 min at 95°C for an initial hot start, followed by 40 cycles of 15 s at 95°C for denaturing, 55 s at 60°C for annealing and extension, and 10 s at 82°C for signal detection. Finally, there was a melting curve analysis step, which was set to be the default condition based on the real-time PCR system. For the PCR master mix, 0.5 µL of each primer at 4 µM, 2.5 µL of EXPRESS SYBR® GreenER™ qPCR SuperMix Universal (2X) (Invitrogen # 11784200, Carlsbad, CA), 0.05 µL ROX reference dye, 0.95 µL DEPC-treated water, and 0.5 µL cDNA were combined. Technical duplicates of PCR analysis were performed for each gene.

The reaction mixtures without cDNA templates served as negative controls. The expression levels of target genes were normalized against the *rbcL* gene.

6.3 Results and discussion

The single-cell laser lysis analysis was performed with the CP-D cell clusters. Before laser lysis, five tubes of pre-lysis media were collected once the cell clusters were trapped in the laser lysis chip. These five tubes of pre-lysis collection presented as the background signal. For every lysed single CP-D cell, the lysates were collected in three 200 µL Eppendorf tubes. The *RPLP1* housekeeping gene was used to validate the lysis result. The validation of single-cell lysis was established upon mRNA analysis on *RPLP1* from each collection. All of the collections were followed through the two-step RT-qPCR procedure as discussed before. In order to validate the accuracy of the qPCR process, an exogenous gene, *rbcL* mRNA, was added into each sample before RNA extraction. The *rbcL* mRNA expression from RT-qPCR can verify if there was any RNA lost or contamination in the extraction or reverse transcription step due to either human errors or other factors. Furthermore, the gene-expression heterogeneity for *RPLP1* could be validated by normalizing with *rbcL* to eliminate systematic errors.

The result in Figure 24 presents the consecutive single CP-D cell lysis collection. The pre-lysis collection from tubes 1 to 5 showed that there were some background issues at the first three tubes; however, the noise went away before the lysis started at tube 6. Most importantly, the background noise was too trivial to affect the cell lysis. During the lysis collection, 13 out of the 14 cells showed positive expression of *RPLP1* mRNA, which indicated the RNA being released from single cells by laser lysis. Additionally, the result

also presents that the efficiency of single cell laser lysis was greater than 90%. Within all 14 cells, 11 cells highly expressed *RPLP1* signals in the first tube and left the second and third in a clear background. This result suggests that the released RNA was collected into the first tube and no cross-contamination was found. Moreover, the heterogeneity of single-cell gene expression was revealed by different expression levels of *RPLP1* among the 13 lysed cells.

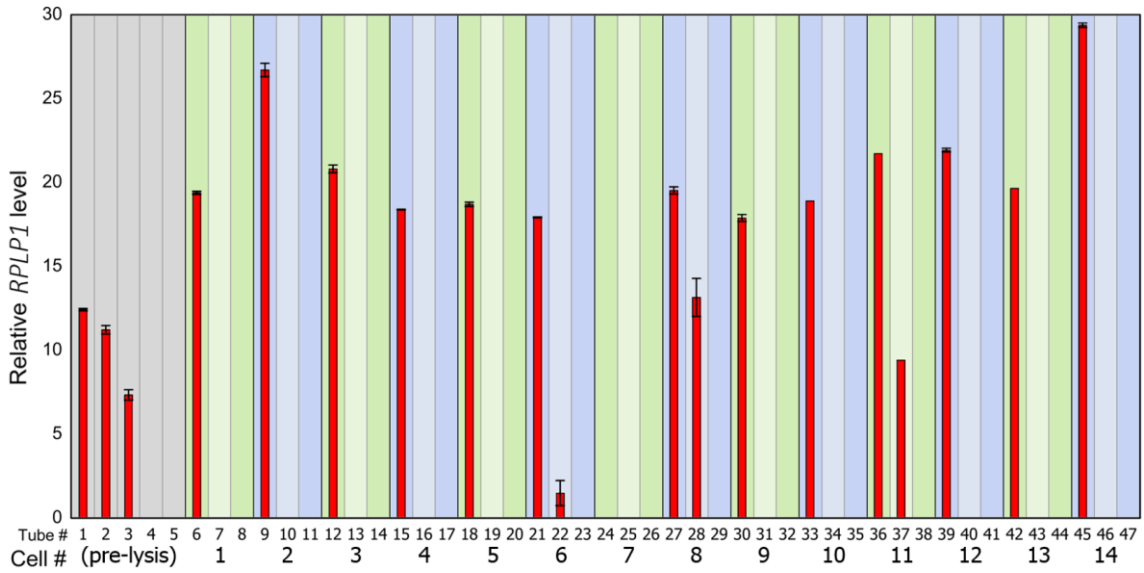

Figure 24. Relative *RPLP1* Level of Single CP-D Cell. Relative *RPLP1* level expression from 14 CP-D cells lysis. Tube 1 to 5 were pre-lysis collection. Lysate from each cell was collected into three tubes accordingly with marked numbers. The red bars indicate *RPLP1* relatively levels across all samples for all cells.

6.4 Conclusion

In the experiment presented, the single cells on the CP-D clusters were lysed individually by using two-photon laser and then the lysates were collected into three Eppendorf tubes for each target cell. The collection was analyzed by the two-step RT-qPCR analysis with the housekeeping gene, *RPLP1*, to validate the lysis result. The single-cell lysis result demonstrates that our development was capable of not only performing single-cell lysis but also analyzing the lysates target with multiple mRNAs at the single-cell level. Most importantly, the system could perform high selective single-cell lysis without compromising the integrity of adjacent cells. The qPCR result also proves that the collection process was highly accurate and specific to distinguish the gene expression for each lysed cell. With this result, our development can elevate single-cell studies to another level, studying the single cells on 3D cell clusters or 3D tissue samples.

7. SINGLE CELL RT-qPCR ANALYSIS ON MIXTURE-CELL CLUSTERS

7.1 Introduction

The cell-to-cell communication signaling and heterogeneity gene expression are critical to study the tumor progression. The tumor progression and metastasis are so complicated that it is necessary to study the variability of gene expression patterns at the single-cell level. This approach will help researchers and scientists to study cancer progression and prognosis for premalignant conditions. This experiment is about using the laser lysis system to lyse mixture-cell clusters and differentiate different cell types by analyzing the endogenous gene. With the result that demonstrates single-cell lysis on CP-D cell clusters, we step forward to lyse and perform two-step RT-qPCR method to analyze different cell lines from mixture cell-lines cell clusters. The CP-D and EPC2 cell clusters were loaded into the laser lysis chip and then lysis was performed sequentially by a two-photon laser system. The lysates were collected for analysis with the two-step RT-qPCR method with *MUC1*, an endogenous gene highly expressed in CP-D cell line.

7.2 Experiment

7.2.1 Experiment preparation

Different from the CP-D experiment, this time two cell clusters, CP-D and EPC2, were loaded separately into the laser lysis chip. As a result, their cluster formation characteristics had to be taken into account. Different cell lines had their physical properties of cluster formation. One example is that the EPC2 clusters were sturdier than CP-D, whose structures were more loose (Figure 22). Therefore, the difference of structure integrity determined the cell loading sequence. The EPC2 cluster cells were loaded into the chip

first followed by CP-D clusters enabling a loading sequence that would trap both clusters securely. This was compared with loading the CP-D clusters first, which resulted in the CP-D clusters most likely being pushed through the cage by the upcoming impact from EPC2 clusters due to their structure integrity difference.

In addition to the loading process, the cluster formation difference also introduces a problem in the lysing step. It is obvious to notice that the structural difference between CP-D and EPC2 clusters (Figure 25). The structure of EPC2 clusters was too tight to identify individual cells. In contrast to the CP-D clusters, the morphology of EPC2 clusters appeared to be more compact and more difficult to target an individual cell. Therefore, the EPC2 clusters were stained with Hoechst® 33342 dye in order to distinguish single cells from the cell clusters. By using Hoechst dye, it is much easier to identify one single cell. Figure 25 shows the trapping result of CP-D and EPC2 cell clusters while EPC2 was stained with Hoechst.

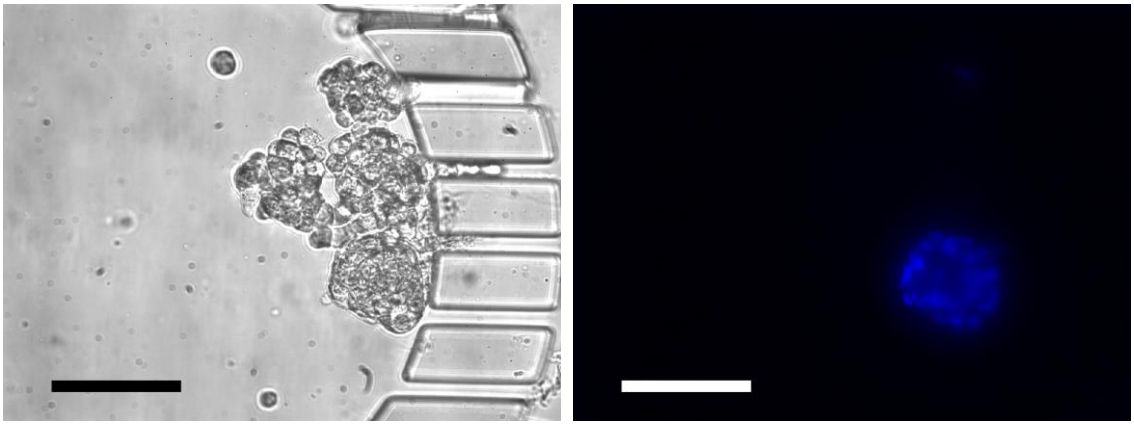

(a) (b)

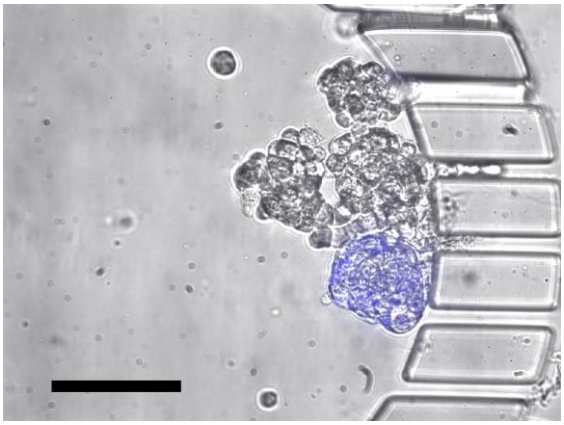

(c)

Figure 25. Trapping CP-D and EPC2 Cell Clusters in Cage. Scale bar: 100 μm. The blue imaging indicates Hoechst stain with EPC2 clusters. (a) Bright field view. (b) Fluorescence imaging. (c) Overlay imaging.

7.2.2 Laser lysis

The laser lysis began after both CP-D and EPC2 clusters were loaded into the laser lysis chip. The lysis progression result is shown in Figure 26. The target cell was marked with an arrow in the figure. The post-lysis result shows that the EPC2 cluster had a crater hole at the target area (Figure 26d), whereas another result shows that the nuclei stain had vanished (Figure 26e). Both results indicate that the target cell was fully lysed. With this result, the single-cell lysis could be performed with one cell line (the CP-D clusters) first, and then collecting the lysate; following by lysing another cell line (the EPC2 clusters) and collecting the lysate accordingly. Figure 27 and 28 show the CP-D and EPC2 cell clusters lysis progression, respectively.

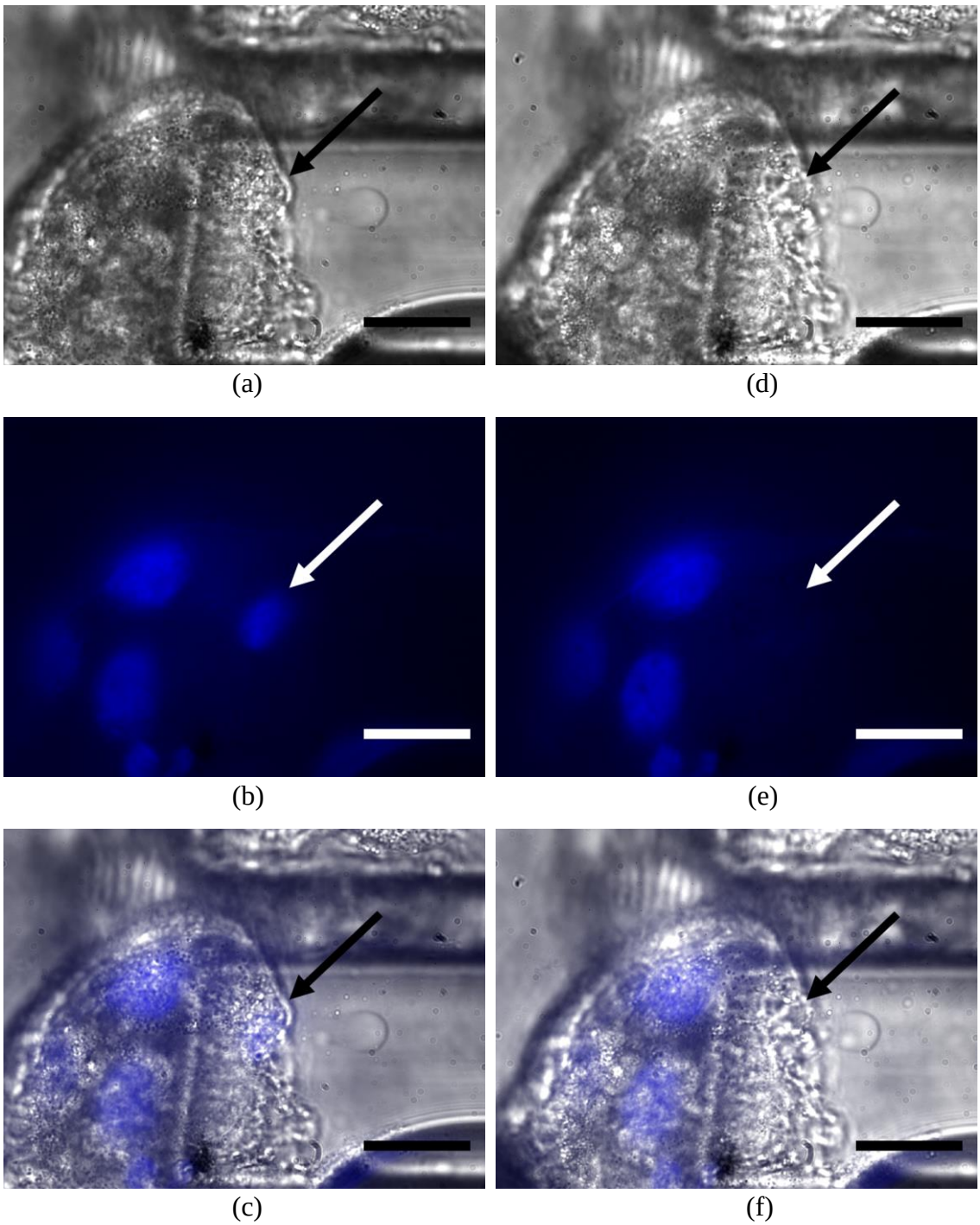

Figure 26. EPC2 Cluster Cell Lysis Process. Scale bar: 20 μm. The blue imaging indicates Hoechst stain with EPC2 clusters. (a)-(c) Before lysis. (d)-(f) After lysis. (a), (d) Target cell under bright field view. (b), (e) Fluorescence imaging. (c), (f) Overlay imaging.

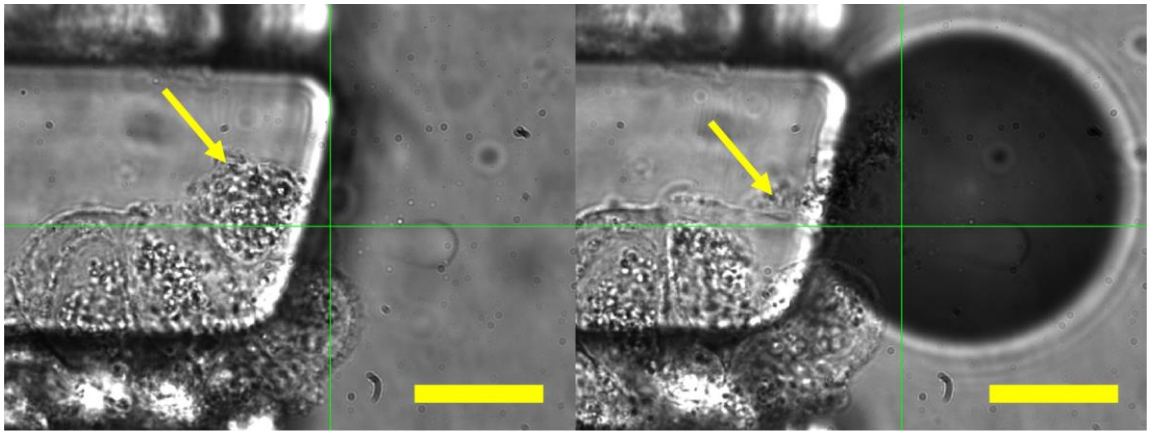

(a) (b)

Figure 27. CP-D Cell Lysis Progression. Scale bar: 20 µm.
(a) Before lysis. (b) After lysis.

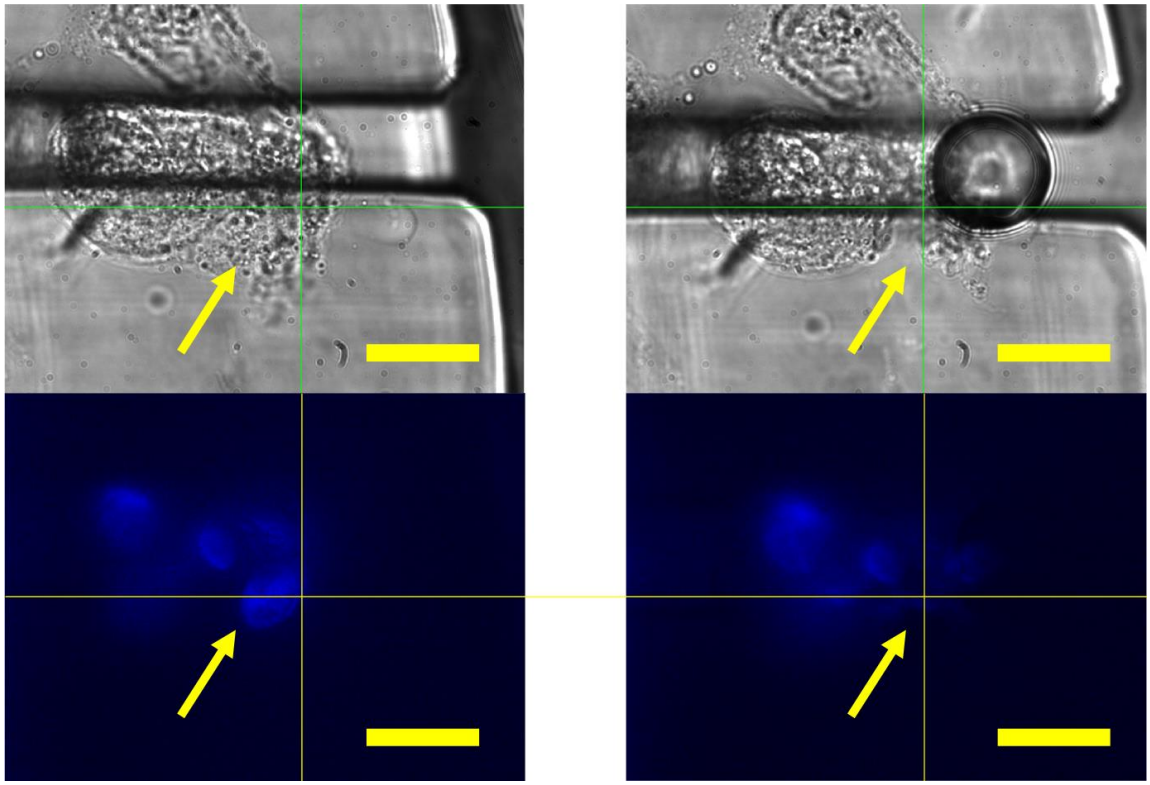

(a) (b)

Figure 28. EPC2 Cell Lysis Progression. Scale bar: 20 µm.
The blue imaging indicates Hoechst stain with EPC2 clusters.
(a) Before lysis. (b) After lysis.

7.2.3 Laser lysis on different tissue samples

In this experiment, different samples other than the cultured tissue were lysed by the laser lysis system. Two samples were used in the laser lysis chip: the mice intestine formalin-fixed paraffin-embedded (FFPE) samples and the patient derived BE tissues.

The FFPE samples were de-paraffinized first then fixed in between two cover slips for lysis; therefore, there was no outlet path for lysate collection. Figure 29 shows the lysis progression of FFPE samples in the dehydrated condition. The dehydration step was performed by soaking the whole sample in ethanol for staining purpose. Next, Figure 30 shows the lysis progression of FFPE samples without dehydration process. The samples were immersed in 1X PBS buffer for 2 min instead of performing a dehydration step.

The patient derived BE tissues were loaded into the laser lysis chip using the same method as discussed before. Figure 31 shows the lysis process of the patient derived BE tissues.

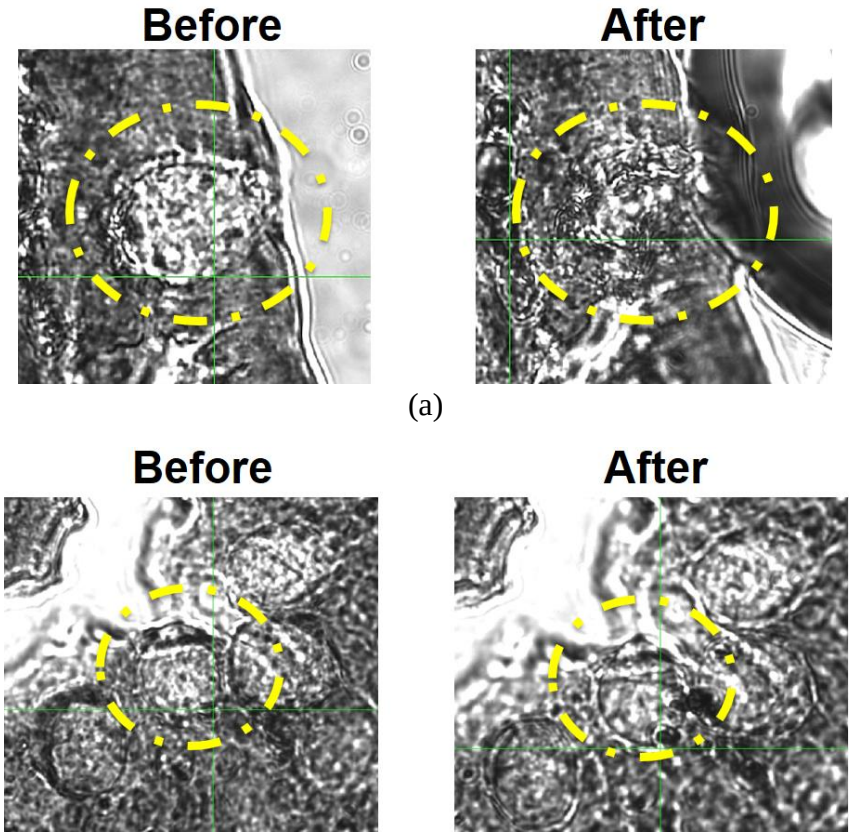

Figure 29. Laser Lysis on the Dehydrated FFPE Samples.
(a) and (b) indicate different locations on the FFPE sample.

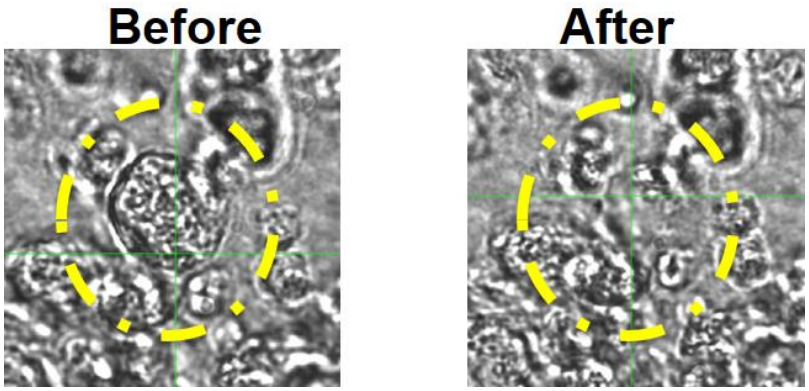

(a)

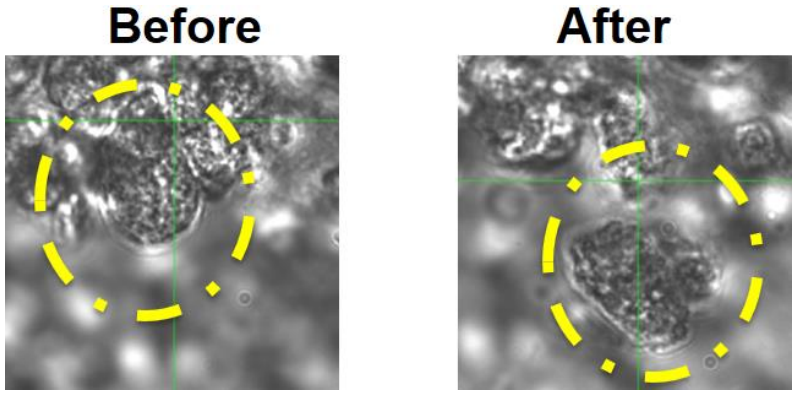

(b)

Figure 30. Laser Lysis on FFPE Samples with Hydration Treatment.
(a) and (b) indicate different locations on the FFPE sample.

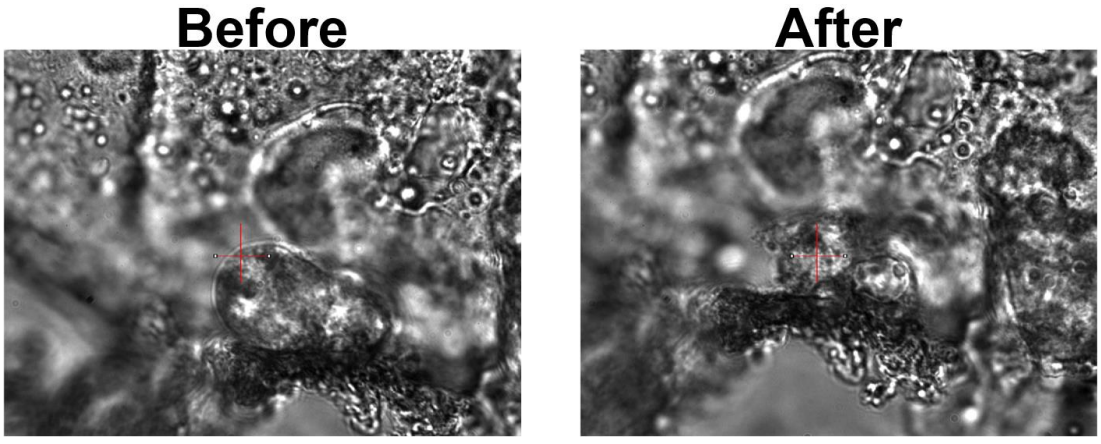

Figure 31. Laser Lysis on Barrett's esophagus Tissue Samples.

7.3 Results and discussion

7.3.1 Mixture-cell clusters

The mixture-cell clusters single-cell lysis followed the same experimental method as single-cell lysis on CP-D (Chapter 6) with the only difference being the loading process as discussed before. We started to lyse one cell on each cell line at a time and collected the released contents accordingly into the Eppendorf tubes. By collecting 200 µL of lysate, all the cell contents were collected. Next, the collected lysate was immediately stored at −80°C in case of RNA degradation. At last, the collection was followed by RNA purification on the same day of laser lysis to minimize the possibility of degradation, followed by the reverse transcription reaction to cDNA template for quantitative PCR analysis.

The single-cell laser lysis spatial recognition with their qPCR results are shown in Figure 32 and 33. To begin with, the target CP-D cell was lysed (Figure 32a) and the lysate was collected concurrently. Next, the collection was analyzed by the two-step RT-qPCR method with the *MUC1* mRNA. The *MUC1* mRNA expression levels were quantified by the cycle threshold (Ct) value, which is defined as the number of cycles required for the fluorescent signal to cross the threshold (Figure32b, 33b). Furthermore, the mRNA authenticity could be validated by the melt curves (Figure 32c, 33c). The target EPC2 cell lysis progression and mRNA results are shown in Figure 33. It is very clear from the amplification plot that the CP-D lysate had a stronger expression level than EPC2 in terms of the *MUC1* mRNA. The melt curves results show even more distinct difference that there was no signal on EPC2 whereas CP-D had spiked signal expression. All data were analyzed and plotted as the box plot in Figure 34.

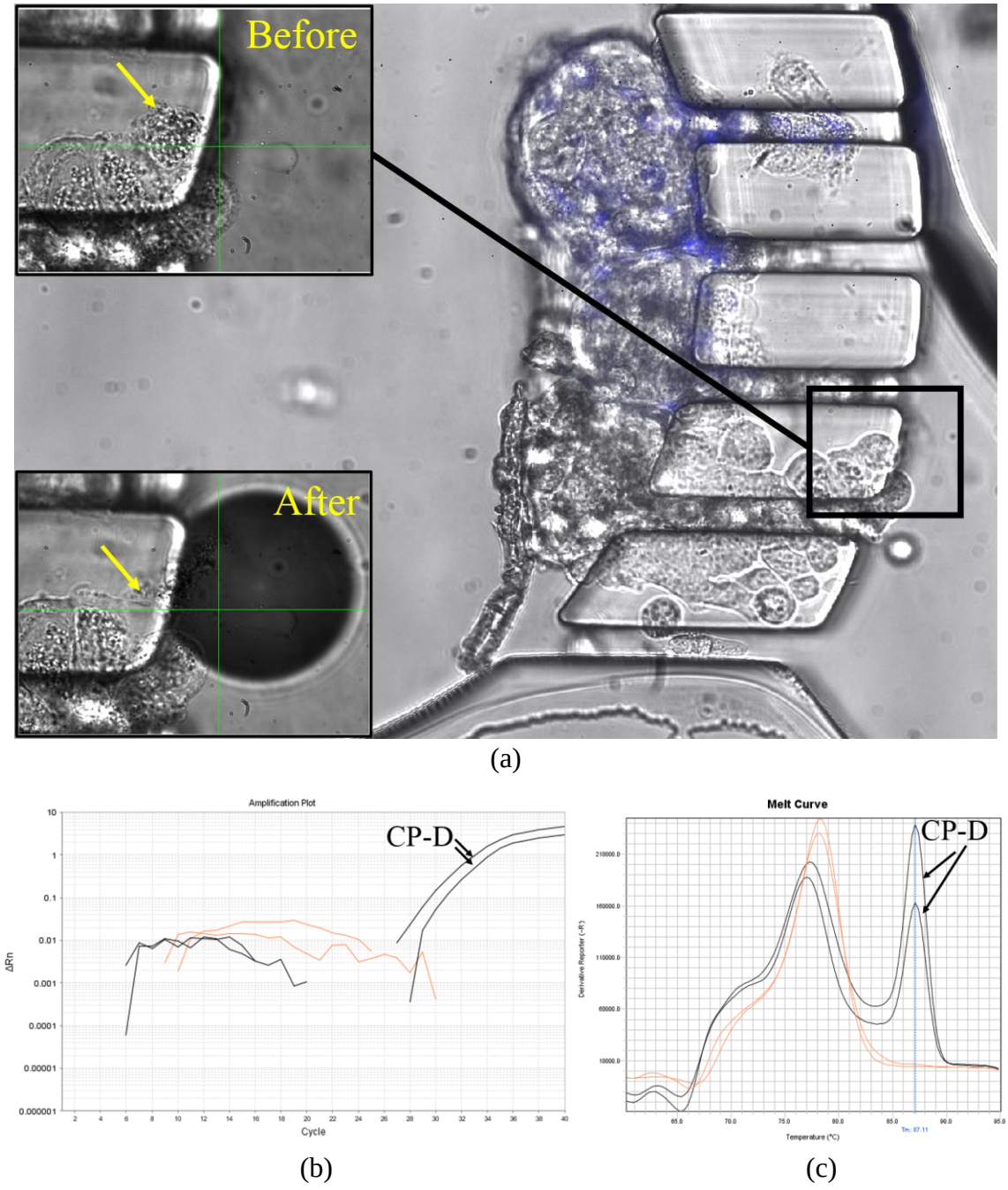

Figure 32. CP-D Cell Lysis Spatial Mapping with mRNA Expression. (a) The CP-D cell lysis progression with spatial location. (b) The CP-D cell mRNA expression signals in amplification plot. (c) The CP-D cell mRNA signals in melt curve.

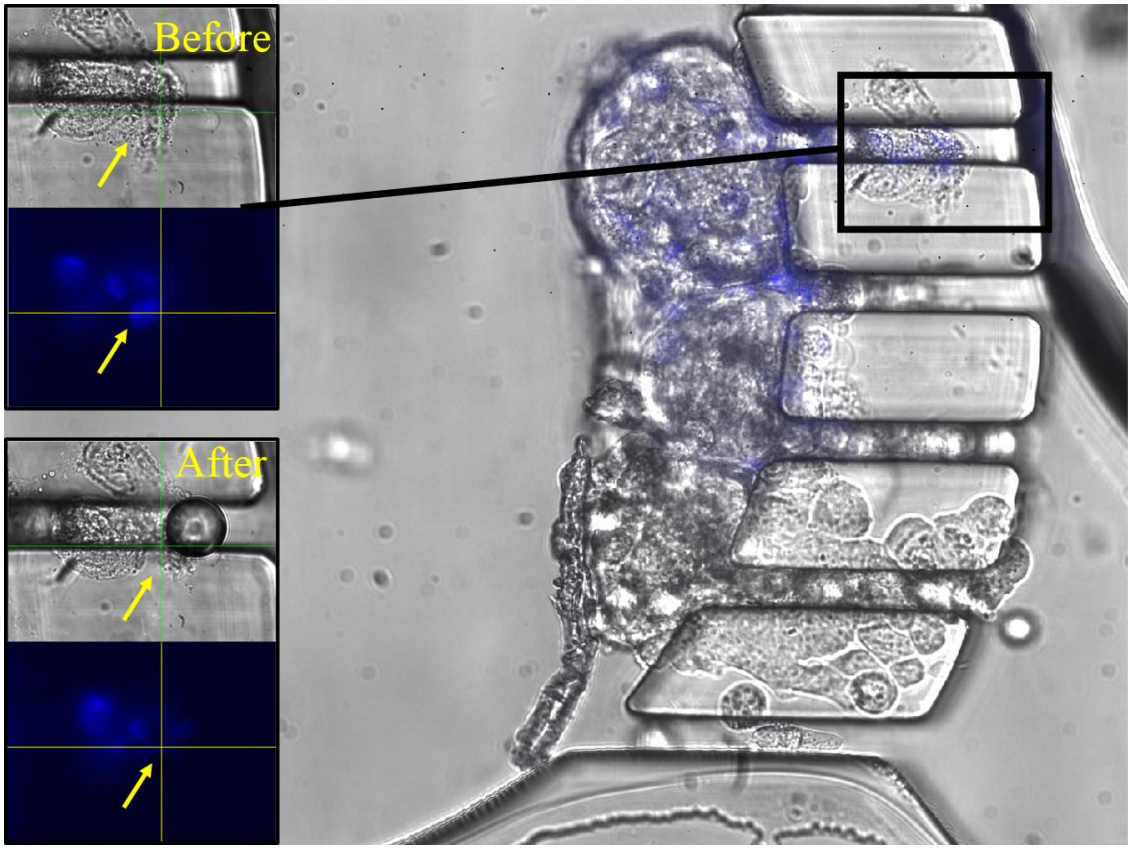

(a)

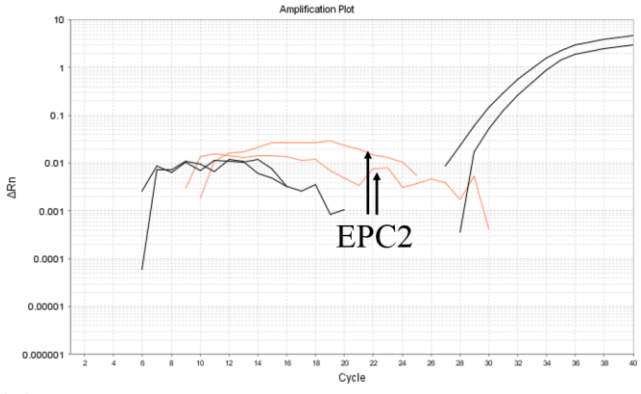

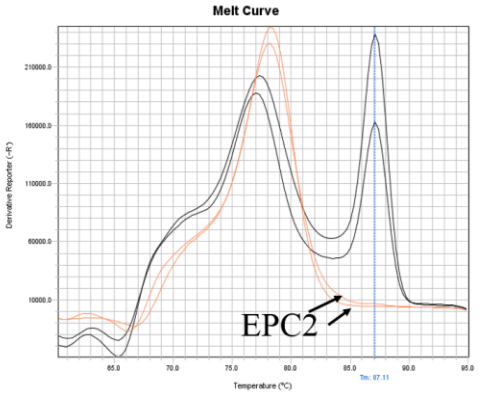

(b) (c)

Figure 33. EPC2 Cell Lysis Spatial Mapping with mRNA Expression. (a) The EPC2 cell lysis progression with spatial location. (b) The EPC2 cell mRNA expression signals in amplification plot. (c) The EPC2 cell mRNA signals in melt curve.

The mixture-cell clusters single-cell lysis result is shown in Figure 34. Three groups: CP-D, EPC2, and pre-lysis collection are shown in Figure 34. The pre-lysis collection was collected before laser lysis which could indicate as the background signal. The result was analyzed by ddCt method (Livak and Schmittgen 2001; Pfaffl 2001), which uses the Ct value of the target gene against the reference gene then normalizes to the calibrator. In detail, the *MUC1* mRNA was selected as the target gene, *RPLP1* as the reference (housekeeping) gene, and four CP-D cells as the calibrator (positive control). By analyzing with the ddCt method, the raw data of CP-D and EPC2 could standardize *MUC1* with *RPLP1* in terms of Ct difference, then normalize with positive control to compare *MUC1* expression between CP-D and EPC2. This method could calibrate *MUC1* from two different cell lines; first to minimize systematic errors due to differences between each cell line, and then to normalize with positive control for comparison in between.

The result in Figure 34 is presented in a box plot. Note that the boxes represent the interquartile range (IQR) between first and third quartiles. The line and dot inside represent the median and mean, respectively. Whiskers denote the lowest and highest values within 1.5 × IQR from the first and third quartiles, respectively. The result clearly demonstrates that the significant difference between CP-D and EPC2 is in terms of the ddCt value, indicating that *MUC1* expression was higher in CP-D compared to the EPC2 cell line which corresponds to bulk-cell expression. For the ddCt value of pre-lysis collection, the influence was too trivial to affect CP-D and EPC2. Furthermore, the result also reveals cell-to-cell gene expression stochasticity from the widely distributed whiskers range among CP-D and EPC2 cell lines. Most importantly, the result shows the difference in median value of CP-D and EPC2 was about 4 which is consistent with the result from bulk-

cell analysis (Table 1), indicating that our system can not only perform laser lysis at a single-cell level with different cell lines, but also maintain high accuracy and specificity.

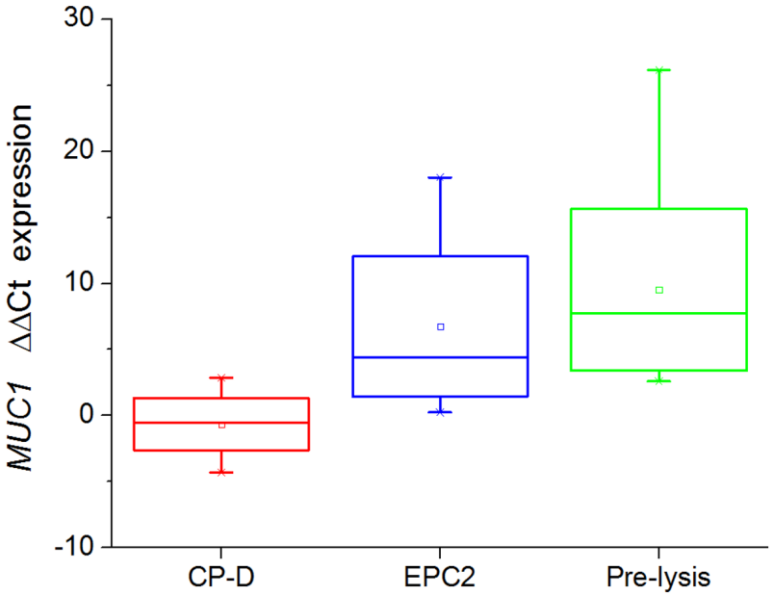

Figure 34. *MUC1* ddCt Expression. Boxes on the graph represent corresponding ddCt and their error range. ddCt was calculated relative to respective controls (*RPLP1* gene and CP-D bulk cells).Graph showing *MUC1* ddCt expression between CP-D, EPC2 samples, and pre-lysis collection (background). This graph shows the CP-D cell line has higher expression of *MUC1* in terms of lower ddCt value while EPC2 has lower *MUC1* expression leads to larger ddCt.

7.3.1.1 Power analysis

Power analysis is needed to determine if the size of the collected samples is enough to ensure the results reach a certain level of power. Additionally, the significance of the results can be revealed by power analysis. Firstly, the bulk cell data (Table 1) was used to determine the estimate sample size required to detect a certain degree of confidence. Secondly, the power was analyzed with our data from mixture-cell clusters. G*Power (Faul et al. 2007), a flexible statistical power analysis program was used to analyze our data.

First, with the data from Table 1, the MUC1 endogenous gene expression patterns were separated into two groups, CP-D and EPC2. By calculating their means and standard deviations, the effect size was determined. The alpha (Type I error) was set as 0.05 and power as 0.95 indicating very powerful experiment. After calculation, the estimate sample size was 5 to reach this significance (Figure 35).

Second, analysis was performed on the data from mixture-cell clusters. The input parameters were data sample sizes, and CP-D, EPC2 data means and standard deviations. Again, we kept alpha (Type I error) at 0.05 then calculated the significance of current parameters. The results show (Figure 36) that the measured sample sizes were large enough to determine the difference between CP-D and EPC2 cell clusters. In fact, 10 successive data samples are enough to ensure an acceptable experimental result (Figure 37).

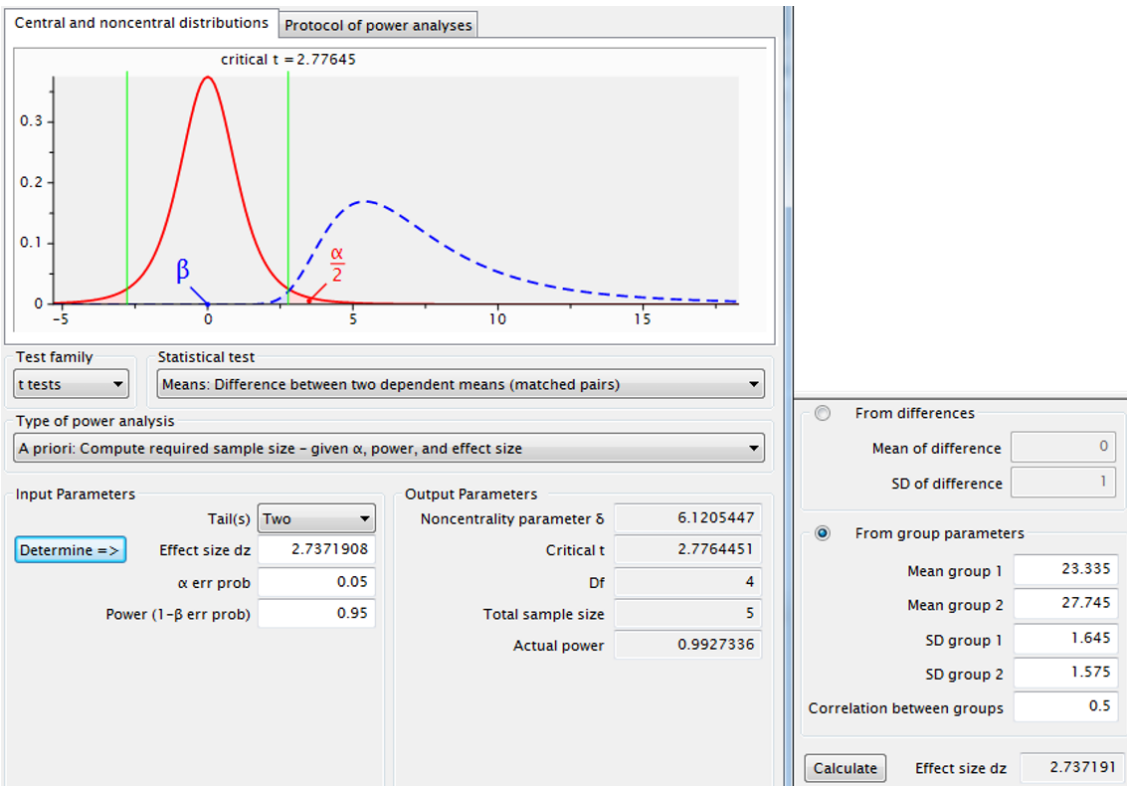

Figure 35. Power Analysis from Table 1.

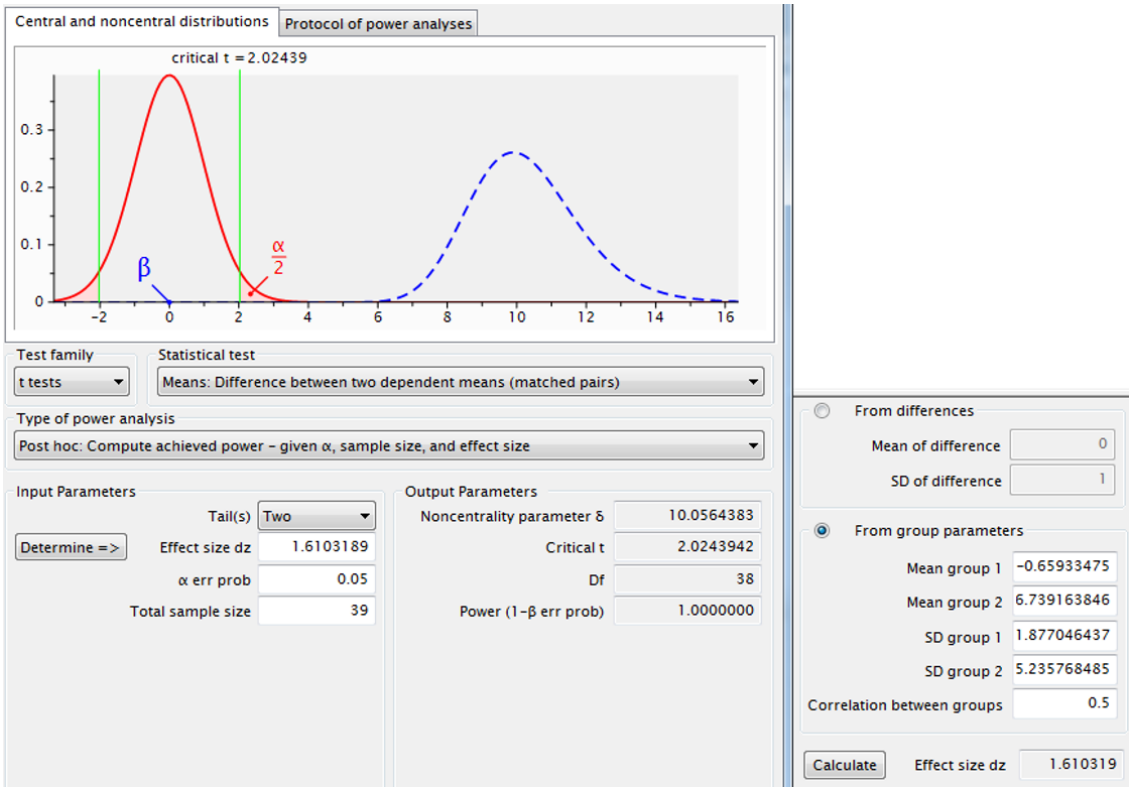

Figure 36. Power Analysis from the Results of Mixture-cell Clusters.

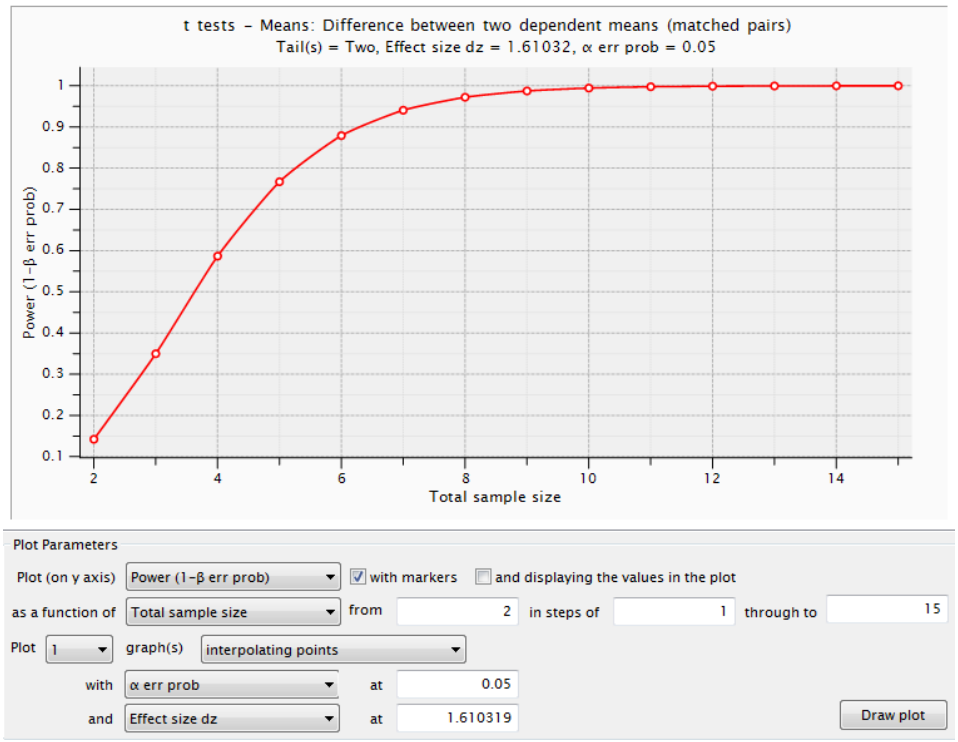

Figure 37. Power as a Function of Sample Size.

7.3.2 Laser lysis on FFPE and BE samples

The FFPE lysis result shows that the cell-to-cell boundaries were easy to identify; however, the laser could not fully lyse dehydrated FFPE samples (Figure 29). It is difficult to perform laser lysis on the rocklike structure due to the dehydration condition. Figure 30 shows the lysis result of the FFPE sample without the dehydration process. One target was fully lysed (Figure 30a), while the other was just separated apart (Figure 30b). In brief, two problems need to be solved in the FFPE sample lysis. Firstly, the lysates could not be collected considering there was no outlet collection path in this experiment design. The FFPE samples could not be loaded into the laser lysis chip due to the structural difference. Secondly, most of the RNA degraded in the FFPE samples due to the modification during fixation and de-paraffin processes (van Beers et al. 2005; Ahlfen et al. 2007; Li et al. 2007; Abramovitz et al. 2008). In general, it will be more difficult to perform laser lysis on the FFPE sample and analyze the lysates at the single-cell level.

The lysis progression of the patient derived BE samples is shown in Figure 31. The major difference between lysing the cultured cell line and the patient derived tissue is the gluey substance called mucus in the cell tissue. The mucus is a sticky, gelatinous substance lines in the lungs, throat, mouth, and esophagus. Mucus is secreted by the mucous membranes and its thick consistency impedes the lysis process. As the result shows, the remaining part of the lysed cell and substances released from the cell were trapped in the thick mucus after cell lysis (Figure 31). Different modifications have been used to eliminate this issue; however, none of them are effective. In order to perform laser lysis on human tissue samples or other biology tissues, it is necessary to overcome this issue.

7.4 Conclusion

We lysed multiple cell lines (CP-D, EPC2) cell clusters simultaneously in the laser lysis chip and analyzed them with a specific endogenous gene, *MUC1*, which was highly expressed only in CP-D cell type. The EPC2 clusters were stained with Hoechst in order to distinguish cell lines during the lysis process. The collection was analyzed by using the two-step RT-qPCR method with *MUC1* mRNA, which only highly expressed in the CP-D cell line. For this reason, it could differentiate these two cell lines. The qPCR results show that there was a huge difference of *MUC1* expression between the CP-D and EPC2 indicating that our development is capable of lysing different cell types and discriminating them with endogenous gene expression at the single-cell level. Additionally, the gene expression of the single cells could be traced back to their original 3D spatial locations thus could conduct a 3D gene expression mapping on the cell cluster.

Two different samples: the FFPE and BE samples were lysed in other experiments. The laser lysis was not effective on the FFPE samples due to the fixation and de-paraffinization process resulting in a rocklike surface. And the laser lysis chip was not compatible with the FFPE sample. As a result, the lysates of the FFPE samples could not be collected for analysis. Furthermore, the fixation and paraffin embedded process could damage the total RNA integrity of the samples. The lysis result of the BE samples shows the mucus had stopped the cells and trapped the released contents.

In summary, results from this study will lead to a greater understanding of cell clusters' gene expression at the single-cell level, and demonstrate laser lysis for a variety of applications.

8. CONCLUSIONS AND FUTURE WORK

8.1 Conclusions and contributions

Based on the results of my research, the major findings and contributions are:

1. A laser lysis chip was designed and developed for performing laser lysis on 3D cell clusters at the single-cell level. The laser lysis chip was built by using soft lithography processes and fabricated with PDMS material, which is commonly used in laboratories. In particular, the laser can access through the 200 μm thick cover glass to perform laser lysis. This chip consists of a) a cage structure for trapping cell clusters; b) microfluidic channels for media and oil perfusion. The media flow carries the released contents from an individual cell while the introduced oil encapsulates the lysate into segments to prevent contamination. More importantly, with this chip, we can perform laser lysis not only on single cell cluster but multiple cell clusters with different cell lines simultaneously.
2. Single-cell gene expression patterns *in situ* in 3D cell clusters have been revealed. We have demonstrated that the laser lysis system can trap cell clusters and lyse individual cells sequentially. The collected lysates are conducted by the two-step RT-qPCR method for multiple gene expression analysis with single-cell resolution. This approach allows single-cell analysis to analyze cellular gene expression and trace back to its original 3D spatial location. These different gene expression patterns are related to cellular interaction, morphology, and microenvironment. Moreover, the different gene expression levels indicate obvious cell-to-cell heterogeneity and thus again emphasize the importance of single-cell analysis.

3. Single-cell gene expression patterns were used to differentiate different cell lines in mixture-cell clusters. Mixture-cell clusters were trapped and serially lysed at the single-cell level from one cell type to another followed by RT-qPCR analysis with the endogenous gene, which is only highly expressed in one cell line. Significant patterns were found in endogenous gene expression between two cell lines, which indicates that the laser lysis system is capable of lysing multiple cell lines at the single-cell level and maintaining its high accuracy and efficiency. Using this approach, the cell-to-cell heterogeneity can be studied not only in one single cell line, but with multicellular systems. This approach can therefore apply to biological tissue samples to study cell-to-cell communications between cancer cells and normal samples.
4. Several characterizations of laser lysis have been made. The laser lysis system was validated by comparing the efficiency with conventional chemical lysis; moreover, the laser-induced cellular stress was analyzed and quantified. The result showed laser lysis had higher mRNA expression and less variances, which indicates it has better signals retrieval rate and higher accuracy than chemical lysis. Next, the cellular stress result was conducted by comparing heat-treated samples to control samples. The result indicated that cellular stress induced by laser lysis was negligible compared to heat-treated samples. Other than that, the laser lysis chip preparation and collection processes had also been optimized for a) preventing cross-contamination; b) higher RNA retrieval rate.
5. A variety of applications for laser lysis were demonstrated: BE tissue samples from Mayo clinic, and the mice intestine FFPE samples were lysed.

With these results, and multiple projects that I have made contributions to, one manuscript is in preparation for publication, one conference paper was published, and I am an author in several co-author publications. All of them are listed below.

1. Kuo-chen Wang, Ganquan Song, Yanqing Tian, Shih-Hui Chao, Hong Wang, Deirdre Meldrum. Micropatterning of Cells into Microwells for Metabolic Profiling. *IEEE EMBS Micro and Nanotechnology in Medicine Conference*. 2014. (Conference)
2. Single cell RT-qPCR analysis *in situ* of 3D cell clusters. *In preparation*.

Co-author:

1. Ganquan Song, Kuo-chen Wang, Benjamin Ueberroth, Fred Lee, Liqiang Zhang, Fengyu Su, Haixin Zhu, Qian Mei, Shih-hui Chao, Laimonas Kelbauskas, Yanqing Tian, Hong Wang, Deirdre Meldrum. Single cell metabolic profiling using multiplexed, photo-patterned fluorescence sensor arrays. *18th International Conference on Miniaturized Systems for Chemistry and Life Sciences. Microtas,* pp. 884–886, 2014. (Conference)
2. Jordan Yaron, Jieying Pan, Tejas Borkar, Kristen Lee, Kuo-Chen Wang, Clifford Anderson, Honor Glenn, Deirdre Meldrum. Automated Cell Counting in a High Density, Polymer-Coated, Live Single Cell Sandwich Microarray. *Microscopy and Microanalysis*, vol. 20, no. S3, pp. 1438–1439, 2014. (Conference)
3. Laimonas Kelbauskas, Rishabh Shetty, Bin Cao, Kuo-chen Wang, Dean Smith, Hong Wang, Joseph Chao, Brian Ashcroft, Margaret Kritzer, Honor Glenn, Roger Johnson, Deirdre Meldrum. Computed tomography for quantitative imaging of live

cancer cells with isotropic 3D spatial resolution. *Engineering and Physical Sciences in Oncology*. 2016. (Poster)

4. Laimonas Kelbauskas, Rishabh Shetty, Bin Cao, Kuo-chen Wang, Dean Smith, Hong Wang, Joseph Chao, Brian Ashcroft, Margaret Kritzer, Honor Glenn, Roger Johnson, Deirdre Meldrum. Computed tomography of living single cells in suspension to achieve isotropic 3D spatial resolution for orientation independent measurement. *Under review*.

8.2 Future work

Although I have built a solid foundation on the development of the laser lysis system and all the goals have been accomplished, there is still room for improvement. To give one example, a more efficient loading method is needed. Currently, the loading method is direct loading from a pipette tip manually. However, it may induce stress to cells and cause background issue. Its efficiency and accuracy is acceptable but it still has potential issues. A potential solution may be to use a glass capillary tip or a pressure driven flow to enhance the efficiency while reducing human errors and stresses to cells.

The other challenge is background signals. There are many causes to introduce background signals. For example, an increment of flow rate in order to shorten operation time will lead to cells being pushed severely against the cage and squeezed through the cage into the downstream flow. In addition, those cells might be trapped in dead volume inside the tubing system. For instance, the lengthy tubing will create dead volumes and micro vortex regions which trap escaped cells and then release at some point in terms of a continuing background noise. Reducing flow rate and optimizing the tubing system as well

as the collection platform can be useful to keep cells from passing through the cage and minimize dead volumes at the same time. Additionally, experiment time can be reduced by improving the tubing system.

Finally, our system could be integrated with Fluidigm. Although the single-cell RT-qPCR method can detect several genes expression at a time, multiplexing measurement is still needed on the long run. By conducting the PCR step with Fluidigm, our throughput of analyzed genes can be significantly increased.

A future proposed development is to design a Micro Total Analysis System (MicroTAS) for single cells laser lysis on 3D cell clusters. The ultimate goal will be to integrate the current laser lysis chip into one on-chip micro-PCR system. However, this will require integration and optimization of the current development. A microchannel for RT-mix reagent can be introduced downstream. The lysates will be mixed with reagents then encapsulated by oil into segments. Next, the outlet connection will be re-designed to integrate with 96-well plates. By using automation technologies, the loading process can automatically dispense into each well. Each well will have the precise amount of encapsulated droplets correlated to one cell. Additionally, the chip layout will be re-designed to shorten the downstream length enabling a faster collection process, decreasing reaction volumes, and minimizing the possibilities of bubble generation. Figure 38 depicts a proposed future approach for Micro-PCR on-chip development.

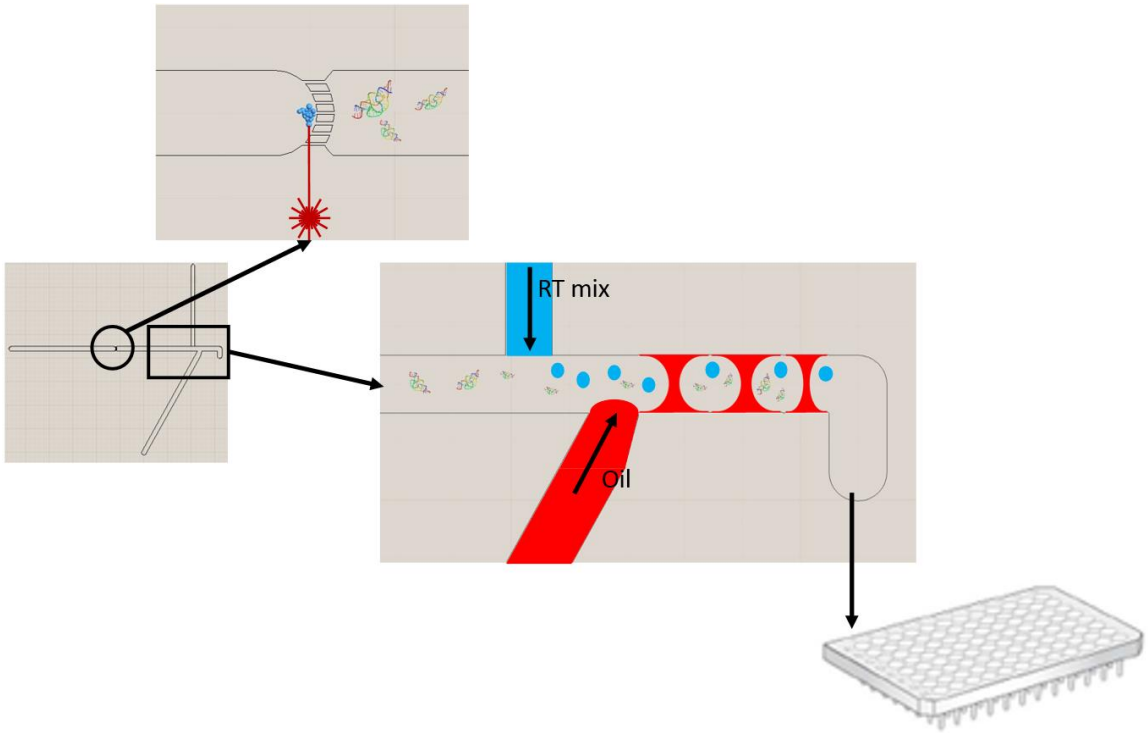

Figure 38. MicroTAS Development. Introduce RT-mix microchannel for performing RT step on-chip. The oil will encapsulate released RNA with RT-mix then dispense into 96-well plate for PCR process.

REFERENCES

Abramovitz, Mark, Maja Ordanic-Kodani, Yuefang Wang, Zhenhong Li, Charles Catzavelos, Mark Bouzyk, George W. Sledge, Carlos S. Moreno, and Brian Leyland-Jones 2008 "Optimization of RNA Extraction from FFPE Tissues for Expression Profiling in the DASL Assay." *BioTechniques* 44(3): 417–423.

Ahlfen, Silke von, Andreas Missel, Klaus Bendrat, and Martin Schlumpberger 2007 "Determinants of RNA Quality from FFPE Samples." *PLOS ONE* 2(12): e1261.

Amann, Rudolf, and Bernhard M. Fuchs 2008 "Single-Cell Identification in Microbial Communities by Improved Fluorescence in Situ Hybridization Techniques." *Nature Reviews Microbiology* 6(5): 339–348.

Anis, Y. H., M. R. Holl, and D. R. Meldrum 2010 "Automated Selection and Placement of Single Cells Using Vision-Based Feedback Control." *IEEE Transactions on Automation Science and Engineering* 7(3): 598–606.

Arnold, W. M., and U. Zimmermann 1988 "Electro-Rotation: Development of a Technique for Dielectric Measurements on Individual Cells and Particles." *Journal of Electrostatics* 21(2–3): 151–191.

Aumiller, G. D., E. A. Chandross, W. J. Tomlinson, and H. P. Weber 1974 "Submicrometer Resolution Replication of Relief Patterns for Integrated Optics." *Journal of Applied Physics* 45(10): 4557–4562.

Banerjee, B., S. Balasubramanian, G. Ananthakrishna, T. V. Ramakrishnan, and G. V. Shivashankar 2004 "Tracking Operator State Fluctuations in Gene Expression in Single Cells." *Biophysical Journal* 86(5): 3052–3059.

Becskei, Attila, Benjamin B. Kaufmann, and Alexander van Oudenaarden 2005 "Contributions of Low Molecule Number and Chromosomal Positioning to Stochastic Gene Expression." *Nature Genetics* 37(9): 937–944.

van Beers, E. H., S. A. Joosse, M. J. Ligtenberg, R. Fles, F. B. L. Hogervorst, S. Verhoef, and P. M. Nederlof 2005 "A Multiplex PCR Predictor for aCGH Success of FFPE Samples." *British Journal of Cancer* 94(2): 333–337.

Brown, Robert B., and Julie Audet 2008 "Current Techniques for Single-Cell Lysis." *Journal of The Royal Society Interface* 5(Suppl 2): S131–S138.

Burghammer, Manfred, Britta Weinhausen, Michael Sztucki, Eva Vergucht, Jan Garrevoet, Stephen Bauters, Maarten De Rijcke, et al. 2015 "X-Ray Fluorescence Imaging of Single-Cell Organisms by Means of Non-Contact Sample Manipulation by Laser-Based Optical Tweezers." *ESRF Experimental Reports EV-118*. http://hdl.handle.net/1854/LU-5955403, accessed July 24, 2016.

Bustin, S. A. 2000
"Absolute Quantification of mRNA Using Real-Time Reverse Transcription Polymerase Chain Reaction Assays." *Journal of Molecular Endocrinology* 25(2): 169–193.

Bustin, S. A., V. Benes, T. Nolan, and M. W. Pfaffl 2005
"Quantitative Real-Time RT-PCR--a Perspective." *Journal of Molecular Endocrinology* 34(3): 597–601.

Cai, Long, Nir Friedman, and X. Sunney Xie 2006
"Stochastic Protein Expression in Individual Cells at the Single Molecule Level." *Nature* 440(7082): 358–362.

Cameron, A. J., B. J. Ott, and W. S. Payne 1985
"The Incidence of Adenocarcinoma in Columnar-Lined (Barrett's) Esophagus." *The New England Journal of Medicine* 313(14): 857–859.

Carlo, Dino Di, Liz Y. Wu, and Luke P. Lee 2006
"Dynamic Single Cell Culture Array." *Lab on a Chip* 6(11): 1445–1449.

Chalfie, M., Y. Tu, G. Euskirchen, W. W. Ward, and D. C. Prasher 1994
"Green Fluorescent Protein as a Marker for Gene Expression." *Science* 263(5148): 802–805.

Charles, Paul T., Veronte R. Stubbs, Carissa M. Soto, Brett D. Martin, Brandy J. White, and Chris R. Taitt 2009 "Reduction of Non-Specific Protein Adsorption Using Poly(ethylene) Glycol (PEG) Modified Polyacrylate Hydrogels In Immunoassays for Staphylococcal Enterotoxin B Detection." *Sensors* 9(1): 645–655.

Chen, Yu-Chih, Patrick N. Ingram, Shamileh Fouladdel, Sean P. McDermott, Ebrahim Azizi, Max S. Wicha, and Euisik Yoon 2016 "High-Throughput Single-Cell Derived Sphere Formation for Cancer Stem-Like Cell Identification and Analysis." *Scientific Reports* 6. http://www.ncbi.nlm.nih.gov/pmc/articles/PMC4904376/, accessed June 28, 2016.

Chen, Yu-Chih, Xia Lou, Zhixiong Zhang, Patrick Ingram, and Euisik Yoon 2015
"High-Throughput Cancer Cell Sphere Formation for Characterizing the Efficacy of Photo Dynamic Therapy in 3D Cell Cultures." *Scientific Reports* 5. http://www.ncbi.nlm.nih.gov/pmc/articles/PMC4495468/, accessed June 28, 2016.

Chung, Jaehoon, Young-Ji Kim, and Euisik Yoon 2011
"Highly-Efficient Single-Cell Capture in Microfluidic Array Chips Using Differential Hydrodynamic Guiding Structures." *Applied Physics Letters* 98(12): 123701.

Colman-Lerner, Alejandro, Andrew Gordon, Eduard Serra, Tina Chin, Orna Resnekov, Drew Endy, C. Gustavo Pesce, and Roger Brent 2005 "Regulated Cell-to-Cell Variation in a Cell-Fate Decision System." *Nature* 437(7059): 699–706.

Convert, Laurence, Vincent Chabot, Pierre-Jean Zermatten, Raymond Hamel Jr., Jean-Pierre Cloarec, Roger Lecomte, Vincent Aimez, and Paul G. Charette 2012 "Passivation of KMPR Microfluidic Channels with Bovine Serum Albumin (BSA) for Improved Hemocompatibility Characterized with Metal-Clad Waveguides." *Sensors and Actuators B: Chemical* 173: 447–454.

David J. Beebe, Glennys A. Mensing, and and Glenn M. Walker 2002
"Physics and Applications of Microfluidics in Biology." *Annual Review of Biomedical Engineering* 4(1): 261–286.

Dittrich, Petra S., and Andreas Manz 2006
"Lab-on-a-Chip: Microfluidics in Drug Discovery." *Nature Reviews. Drug Discovery* 5(3): 210–218.

Drewitz, D. J., R. E. Sampliner, and H. S. Garewal 1997
"The Incidence of Adenocarcinoma in Barrett's Esophagus: A Prospective Study of 170 Patients Followed 4.8 Years." *The American Journal of Gastroenterology* 92(2): 212–215.

Fan, Jean, Neeraj Salathia, Rui Liu, Gwendolyn E. Kaeser, Yun C. Yung, Joseph L. Herman, Fiona Kaper, et al. 2016 "Characterizing Transcriptional Heterogeneity through Pathway and Gene Set Overdispersion Analysis." *Nature Methods* 13(3): 241–244.

Faul, Franz, Edgar Erdfelder, Albert-Georg Lang, and Axel Buchner 2007
"G*Power 3: A Flexible Statistical Power Analysis Program for the Social, Behavioral, and Biomedical Sciences." *Behavior Research Methods* 39(2): 175–191.

Gao, Weimin, Weiwen Zhang, and Deirdre R. Meldrum 2011
"RT-qPCR Based Quantitative Analysis of Gene Expression in Single Bacterial Cells." *Journal of Microbiological Methods* 85(3): 221–227.

Gould, Stephen J., and Suresh Subramani 1988
"Firefly Luciferase as a Tool in Molecular and Cell Biology." *Analytical Biochemistry* 175(1): 5–13.

Guet, Călin C., Luke Bruneaux, Taejin L. Min, Dan Siegal-Gaskins, Israel Figueroa, Thierry Emonet, and Philippe Cluzel 2008 "Minimally Invasive Determination of mRNA Concentration in Single Living Bacteria." *Nucleic Acids Research* 36(12): e73.

Hansen, Carl L., Emmanuel Skordalakes, James M. Berger, and Stephen R. Quake 2002 "A Robust and Scalable Microfluidic Metering Method That Allows Protein Crystal Growth by Free Interface Diffusion." *Proceedings of the National Academy of Sciences of the United States of America* 99(26): 16531–16536.

Harada, Hideki, Hiroshi Nakagawa, Kenji Oyama, Munenori Takaoka, Claudia D. Andl, Birgit Jacobmeier, Alexander von Werder, Gregory H. Enders, Oliver G. Opitz, and Anil K. Rustgi 2003 "Telomerase Induces Immortalization of Human Esophageal Keratinocytes without p16INK4a Inactivation." *Molecular Cancer Research* 1(10): 729–738.

Hartshorn, Cristina, Judith J. Eckert, Odelya Hartung, and Lawrence J. Wangh 2007 "Single-Cell Duplex RT-LATE-PCR Reveals Oct4 and XistRNA Gradients in 8-Cell Embryos." *BMC Biotechnology* 7: 87.

He, J.-Q., A. J. Sandford, I.-M. Wang, S. Stepaniants, D. A. Knight, A. Kicic, S. M. Stick, and P. D. Paré 2008 "Selection of Housekeeping Genes for Real-Time PCR in Atopic Human Bronchial Epithelial Cells." *European Respiratory Journal* 32(3): 755–762.

Heid, C. A., J. Stevens, K. J. Livak, and P. M. Williams 1996 "Real Time Quantitative PCR." *Genome Research* 6(10): 986–994.

Hellman, Amy N., Kaustubh R. Rau, Helen H. Yoon, and Vasan Venugopalan 2008 "Biophysical Response to Pulsed Laser Microbeam-Lnduced Cell Lysis and Molecular Delivery." *Journal of Biophotonics* 1(1): 24–35.

Helmchen, Fritjof, and Winfried Denk 2005 "Deep Tissue Two-Photon Microscopy." *Nature Methods* 2(12): 932–940.

Hoshino, Hideto, Yoshihiro Nakajima, and Yoshihiro Ohmiya 2007 "Luciferase-YFP Fusion Tag with Enhanced Emission for Single-Cell Luminescence Imaging." *Nature Methods* 4(8): 637–639.

Howlader et al. 2016 "SEER Cancer Statistics Review, 1975-2013," *National Cancer Institute.* http://seer.cancer.gov/csr/1975_2013/.

Huang, Kuo-Wei, Yi-Chien Wu, Ji-Ann Lee, and Pei-Yu Chiou 2013 "Microfluidic Integrated Optoelectronic Tweezers for Single-Cell Preparation and Analysis." *Lab on a Chip* 13(18): 3721–3727.

Huang, Nien-Tsu, Hua-Li Zhang, Meng-Ting Chung, Jung Hwan Seo,
and Katsuo Kurabayashi 2014 "Recent Advancements in Optofluidics-Based Single-Cell Analysis: Optical on-Chip Cellular Manipulation, Treatment, and Property Detection." *Lab on a Chip* 14(7): 1230–1245.

Irimia, Daniel, Ronald G. Tompkins, and Mehmet Toner 2004
"Single-Cell Chemical Lysis in Picoliter-Scale Closed Volumes Using a Microfabricated Device." *Analytical Chemistry* 76(20): 6137–6143.

Jäättelä, Marja, Dorte Wissing, Klaus Kokholm, Tuula Kallunki, and Mikala Egeblad 1998
"Hsp70 Exerts Its Anti - apoptotic Function Downstream of caspase - 3 - like Proteases." *The EMBO Journal* 17(21): 6124–6134.

Jäättelä, M, D Wissing, P A Bauer, and G C Li 1992
"Major Heat Shock Protein hsp70 Protects Tumor Cells from Tumor Necrosis Factor Cytotoxicity." *The EMBO Journal* 11(10): 3507–3512.

Jen, Chun-Ping, Ju-Hsiu Hsiao, and Nikolay A. Maslov 2012
"Single-Cell Chemical Lysis on Microfluidic Chips with Arrays of Microwells." *Sensors (Basel, Switzerland)* 12(1): 347–358.

Kelly, C. D., and Otto Rahn 1932
"The Growth Rate of Individual Bacterial Cells." *Journal of Bacteriology* 23(2): 147–153.

Kim, R., J. L. Weissfeld, J. C. Reynolds, and L. H. Kuller 1997
"Etiology of Barrett's Metaplasia and Esophageal Adenocarcinoma." *Cancer Epidemiology Biomarkers & Prevention* 6(5): 369–377.

Klein, Allon M., Linas Mazutis, Ilke Akartuna, Naren Tallapragada, Adrian Veres,
Victor Li, Leonid Peshkin, David A. Weitz, and Marc W. Kirschner 2015 "Droplet Barcoding for Single-Cell Transcriptomics Applied to Embryonic Stem Cells." *Cell* 161(5): 1187–1201.

Kuang, Yina, Israel Biran, and David R. Walt 2004
"Simultaneously Monitoring Gene Expression Kinetics and Genetic Noise in Single Cells by Optical Well Arrays." *Analytical Chemistry* 76(21): 6282–6286.

Kubista, Mikael, José Manuel Andrade, Martin Bengtsson, Amin Forootan, Jiri Jonák,
Kristina Lind, Radek Sindelka, et al. 2006 "The Real-Time Polymerase Chain Reaction." *Molecular Aspects of Medicine* 27(2–3): 95–125.

Lai, S. L., D. Johnson, and R. Westerman 2006
"Aspect Ratio Dependent Etching Lag Reduction in Deep Silicon Etch Processes." *Journal of Vacuum Science & Technology A* 24(4): 1283–1288.

Le, Thuc T., Thierry Emonet, Sebastien Harlepp, Calin C. Guet, and Philippe Cluzel 2006 "Dynamical Determinants of Drug-Inducible Gene Expression in a Single Bacterium." *Biophysical Journal* 90(9): 3315–3321.

Levsky, Jeffrey M., Shailesh M. Shenoy, Rossanna C. Pezo, and Robert H. Singer 2002 "Single-Cell Gene Expression Profiling." *Science (New York, N.Y.)* 297(5582): 836–840.

Levsky, Jeffrey M., and Robert H. Singer 2003 "Fluorescence in Situ Hybridization: Past, Present and Future." *Journal of Cell Science* 116(14): 2833–2838.

Li, G C, and Z Werb 1982 "Correlation between Synthesis of Heat Shock Proteins and Development of Thermotolerance in Chinese Hamster Fibroblasts." *Proceedings of the National Academy of Sciences of the United States of America* 79(10): 3218–3222.

Li, Jinghuan, Paul Smyth, Richard Flavin, Susanne Cahill, Karen Denning, Sinead Aherne, Simone M Guenther, John J O'Leary, and Orla Sheils 2007 "Comparison of miRNA Expression Patterns Using Total RNA Extracted from Matched Samples of Formalin-Fixed Paraffin-Embedded (FFPE) Cells and Snap Frozen Cells." *BMC Biotechnology* 7: 36.

Li, Yongzhong, Hansa Thompson, Courtney Hemphill, Fan Hong, Jessica Forrester, Roger H. Johnson, Weiwen Zhang, and Deirdre R. Meldrum 2010 "An Improved One-Tube RT-PCR Protocol for Analyzing Single-Cell Gene Expression in Individual Mammalian Cells." *Analytical and Bioanalytical Chemistry* 397(5): 1853–1859.

Lidstrom, Mary E., and Deirdre R. Meldrum 2003 "Life-on-a-Chip." *Nature Reviews Microbiology* 1(2): 158–164.

Lindqvist, Niclas, Manuel Vidal-Sanz, and Finn Hallböök 2002 "Single Cell RT-PCR Analysis of Tyrosine Kinase Receptor Expression in Adult Rat Retinal Ganglion Cells Isolated by Retinal Sandwiching." *Brain Research. Brain Research Protocols* 10(2): 75–83.

Lindsay, Stuart, Peiming Zhang, and Yanan Zhao 2015 "Systems, Apparatuses and Methods for Reading an Amino Acid Sequence." http://www.google.com/patents/US20150010935, accessed September 28, 2016.

Livak, K. J., and T. D. Schmittgen 2001 "Analysis of Relative Gene Expression Data Using Real-Time Quantitative PCR and the 2(-Delta Delta C(T)) Method." *Methods (San Diego, Calif.)* 25(4): 402–408.

Lubeck, Eric, and Long Cai 2012
"Single-Cell Systems Biology by Super-Resolution Imaging and Combinatorial Labeling." *Nature Methods* 9(7): 743–748.

Lubeck, Eric, Ahmet F. Coskun, Timur Zhiyentayev, Mubhij Ahmad, and Long Cai 2014
"Single-Cell in Situ RNA Profiling by Sequential Hybridization." *Nature Methods* 11(4): 360–361.

Maloney, Peter C., and Boris Rotman 1973
"Distribution of Suboptimally Induced β-D-Galactosidase in Escherichia Coli." *Journal of Molecular Biology* 73(1): 77–91.

Marcus, Joshua S., W. French Anderson, and Stephen R. Quake 2006
"Microfluidic Single-Cell mRNA Isolation and Analysis." *Analytical Chemistry* 78(9): 3084–3089.

Meng, Long, Feiyan Cai, Zidong Zhang, Lili Niu, Qiaofeng Jin, Fei Yan, Junru Wu, Zhanhui Wang, and Hairong Zheng 2011 "Transportation of Single Cell and Microbubbles by Phase-Shift Introduced to Standing Leaky Surface Acoustic Waves." *Biomicrofluidics* 5(4): 44104.

Minner, Frédéric, and Yves Poumay 2009
"Candidate Housekeeping Genes Require Evaluation before Their Selection for Studies of Human Epidermal Keratinocytes." *The Journal of Investigative Dermatology* 129(3): 770–773.

Moter, Annette, and Ulf B Göbel 2000
"Fluorescence in Situ Hybridization (FISH) for Direct Visualization of Microorganisms." *Journal of Microbiological Methods* 41(2): 85–112.

Murata, Tatsuya, Tomoyuki Yasukawa, Hitoshi Shiku, and Tomokazu Matsue 2009
"Electrochemical Single-Cell Gene-Expression Assay Combining Dielectrophoretic Manipulation with Secreted Alkaline Phosphatase Reporter System." *Biosensors and Bioelectronics* 25(4): 913–919.

Newman, John R. S., Sina Ghaemmaghami, Jan Ihmels, David K. Breslow, Matthew Noble, Joseph L. DeRisi, and Jonathan S. Weissman 2006 "Single-Cell Proteomic Analysis of S. Cerevisiae Reveals the Architecture of Biological Noise." *Nature* 441(7095): 840–846.

Nolan, Tania, Rebecca E. Hands, and Stephen A. Bustin 2006
"Quantification of mRNA Using Real-Time RT-PCR." *Nature Protocols* 1(3): 1559–1582.

Ocvirk, G., H. Salimi-Moosavi, R. J. Szarka, E. A. Arriaga, P. E. Andersson, R. Smith, N. J. Dovichi, and D. J. Harrison 2004 "Beta;-Galactosidase Assays of Single-Cell Lysates on a Microchip: A Complementary Method for Enzymatic Analysis of Single Cells." *Proceedings of the IEEE* 92(1): 115–125.

Palanca-Wessels, M. Corinna, Michael T. Barrett, Patricia C. Galipeau, Katherine L. Rohrer, Brian J. Reid, and Peter S. Rabinovitch 1998 "Genetic Analysis of Long-Term Barrett's Esophagus Epithelial Cultures Exhibiting Cytogenetic and Ploidy Abnormalities." *Gastroenterology* 114(2): 295–304.

Pedraza, Juan M., and Alexander van Oudenaarden 2005 "Noise Propagation in Gene Networks." *Science* 307(5717): 1965–1969.

Pernthaler, Annelie, and Rudolf Amann 2004 "Simultaneous Fluorescence In Situ Hybridization of mRNA and rRNA in Environmental Bacteria." *Applied and Environmental Microbiology* 70(9): 5426–5433.

Pfaffl, M. W. 2001 "A New Mathematical Model for Relative Quantification in Real-Time RT-PCR." *Nucleic Acids Research* 29(9): e45.

Quinto-Su, Pedro A., Hsuan-Hong Lai, Helen H. Yoon, Christopher E. Sims, Nancy L. Allbritton, and Vasan Venugopalan 2008 "Examination of Laser Microbeam Cell Lysis in a PDMS Microfluidic Channel Using Time-Resolved Imaging." *Lab on a Chip* 8(3): 408–414.

Ramsey, R. S., and J. M. Ramsey 1997 "Generating Electrospray from Microchip Devices Using Electroosmotic Pumping." *Analytical Chemistry* 69(6): 1174–1178.

Rau, Kaustubh R., Arnold Guerra Iii, Alfred Vogel, and Vasan Venugopalan 2004 "Investigation of Laser-Induced Cell Lysis Using Time-Resolved Imaging." *Applied Physics Letters* 84(15): 2940–2942.

Rau, Kaustubh R., Pedro A. Quinto-Su, Amy N. Hellman, and Vasan Venugopalan 2006 "Pulsed Laser Microbeam-Induced Cell Lysis: Time-Resolved Imaging and Analysis of Hydrodynamic Effects." *Biophysical Journal* 91(1): 317–329.

Rosenfeld, Nitzan, Jonathan W. Young, Uri Alon, Peter S. Swain, and Michael B. Elowitz 2005 "Gene Regulation at the Single-Cell Level." *Science* 307(5717): 1962–1965.

Sasuga, Yasuhiro, Tomoyuki Iwasawa, Kayoko Terada, Yoshihiro Oe, Hiroyuki Sorimachi, Osamu Ohara, and Yoshie Harada 2008 "Single-Cell Chemical Lysis Method for Analyses of Intracellular Molecules Using an Array of Picoliter-Scale Microwells." *Analytical Chemistry* 80(23): 9141–9149.

Sharma, Prateek, Kenneth McQuaid, John Dent, M. Brian Fennerty, Richard Sampliner, Stuart Spechler, Alan Cameron, et al. 2004 "A Critical Review of the Diagnosis and Management of Barrett's Esophagus: The AGA Chicago Workshop." *Gastroenterology* 127(1): 310–330.

Shoemaker, Glen K., Justin Lorieau, Leon H. Lau, C. Stewart Gillmor, and Monica M. Palcic 2005 "Multiple Sampling in Single-Cell Enzyme Assays Using CE-Laser-Induced Fluorescence to Monitor Reaction Progress." *Analytical Chemistry* 77(10): 3132–3137.

Sia, Samuel K., and George M. Whitesides 2003 "Microfluidic Devices Fabricated in Poly(dimethylsiloxane) for Biological Studies." *Electrophoresis* 24(21): 3563–3576.

Siegel, Rebecca L., Kimberly D. Miller, and Ahmedin Jemal 2016 "Cancer Statistics, 2016." *CA: A Cancer Journal for Clinicians* 66(1): 7–30.

Siegele, Deborah A., and James C. Hu 1997 "Gene Expression from Plasmids Containing the araBAD Promoter at Subsaturating Inducer Concentrations Represents Mixed Populations." *Proceedings of the National Academy of Sciences* 94(15): 8168–8172.

Soeller, C., and M. B. Cannell 1999 "Two-Photon Microscopy: Imaging in Scattering Samples and Three-Dimensionally Resolved Flash Photolysis." *Microscopy Research and Technique* 47(3): 182–195.

Spudich, John L., and D. E. Koshland 1976 "Non-Genetic Individuality: Chance in the Single Cell." *Nature* 262(5568): 467–471.

Squirrell, J. M., D. L. Wokosin, J. G. White, and B. D. Bavister 1999 "Long-Term Two-Photon Fluorescence Imaging of Mammalian Embryos without Compromising Viability." *Nature Biotechnology* 17(8): 763–767.

Steg, Adam, Wenquan Wang, Carmelo Blanquicett, Jessica M. Grunda, Isam A. Eltoum, Kangsheng Wang, Donald J. Buchsbaum, et al. 2006 "Multiple Gene Expression Analyses in Paraffin-Embedded Tissues by TaqMan Low-Density Array: Application to Hedgehog and Wnt Pathway Analysis in Ovarian Endometrioid Adenocarcinoma." *The Journal of Molecular Diagnostics* 8(1): 76–83.

Stewart, Philip S., and Michael J. Franklin 2008 "Physiological Heterogeneity in Biofilms." *Nature Reviews Microbiology* 6(3): 199–210.

Strovas, Tim J., and Mary E. Lidstrom 2009
"Population Heterogeneity in Methylobacterium Extorquens AM1." *Microbiology* 155(6): 2040–2048.

Strovas, Tim J., Linda M. Sauter, Xiaofeng Guo, and Mary E. Lidstrom 2007
"Cell-to-Cell Heterogeneity in Growth Rate and Gene Expression in Methylobacterium Extorquens AM1." *Journal of Bacteriology* 189(19): 7127–7133.

Stumpf, F., J. Schoendube, A. Gross, C. Rath, S. Niekrawietz, P. Koltay, and G. Roth 2015
"Single-Cell PCR of Genomic DNA Enabled by Automated Single-Cell Printing for Cell Isolation." *Biosensors and Bioelectronics* 69: 301–306.

Svoboda, K., and S. M. Block 1994
"Biological Applications of Optical Forces." *Annual Review of Biophysics and Biomolecular Structure* 23: 247–285.

Tillberg, Paul W., Fei Chen, Kiryl D. Piatkevich, Yongxin Zhao, Chih-Chieh Jay Yu, Brian P. English, Linyi Gao, et al. 2016 "Protein-Retention Expansion Microscopy of Cells and Tissues Labeled Using Standard Fluorescent Proteins and Antibodies." *Nature Biotechnology* 34(9): 987–992.

Ungai-Salánki, Rita, Tamás Gerecsei, Péter Fürjes, Norbert Orgovan, Noémi Sándor, Eszter Holczer, Robert Horvath, and Bálint Szabó 2016 "Automated Single Cell Isolation from Suspension with Computer Vision." *Scientific Reports 6*. http://www.ncbi.nlm.nih.gov/pmc/articles/PMC4746594/, accessed July 22, 2016.

Vogel, A., J. Noack, K. Nahen, D. Theisen, S. Busch, U. Parlitz, D. X. Hammer, G. D. Noojin, B. A. Rockwell, and R. Birngruber 1999 "Energy Balance of Optical Breakdown in Water at Nanosecond to Femtosecond Time Scales." *Applied Physics B* 68(2): 271–280.

Voldman, J., M. Toner, M. L. Gray, and M. A. Schmidt 2003
"Design and Analysis of Extruded Quadrupolar Dielectrophoretic Traps." *Journal of Electrostatics* 57(1): 69–90.

Wacker, Michael J., Michelle M. Tehel, and Philip M. Gallagher 2008
"Technique for Quantitative RT-PCR Analysis Directly from Single Muscle Fibers." *Journal of Applied Physiology (Bethesda, Md.*: 1985) 105(1): 308–315.

Wang, Ting, Zong-An Liang, Andrew J. Sandford, Xing-Yu Xiong, Yin-Yin Yang, Yu-Lin Ji, and Jian-Qing He 2012 "Selection of Suitable Housekeeping Genes for Real-Time Quantitative PCR in CD4 + Lymphocytes from Asthmatics with or without Depression." *PLOS ONE* 7(10): e48367.

Werdich, Andreas A., Eduardo A. Lima, Borislav Ivanov, Igor Ges, Mark E. Anderson, John P. Wikswo, and Franz J. Baudenbacher 2004 "A Microfluidic Device to Confine a Single Cardiac Myocyte in a Sub-Nanoliter Volume on Planar Microelectrodes for Extracellular Potential Recordings." *Lab on a Chip* 4(4): 357–362.

Wet, J. R. de, K. V. Wood, M. DeLuca, D. R. Helinski, and S. Subramani 1987 "Firefly Luciferase Gene: Structure and Expression in Mammalian Cells." *Molecular and Cellular Biology* 7(2): 725–737.

Wheeler, Aaron R., William R. Throndset, Rebecca J. Whelan, Andrew M. Leach, Richard N. Zare, Yish Hann Liao, Kevin Farrell, Ian D. Manger, and Antoine Daridon 2003 "Microfluidic Device for Single-Cell Analysis." *Analytical Chemistry* 75(14): 3581–3586.

White, Adam K., Michael VanInsberghe, Oleh I. Petriv, Mani Hamidi, Darek Sikorski, Marco A. Marra, James Piret, Samuel Aparicio, and Carl L. Hansen 2011 "High-Throughput Microfluidic Single-Cell RT-qPCR." *Proceedings of the National Academy of Sciences* 108(34): 13999–14004.

Whitesides, George M. 2006 "The Origins and the Future of Microfluidics." *Nature* 442(7101): 368–373.

Wolf, Marc, David Juncker, Bruno Michel, Patrick Hunziker, and Emmanuel Delamarche 2004 "Simultaneous Detection of C-Reactive Protein and Other Cardiac Markers in Human Plasma Using Micromosaic Immunoassays and Self-Regulating Microfluidic Networks." *Biosensors & Bioelectronics* 19(10): 1193–1202.

Yu, Ji, Jie Xiao, Xiaojia Ren, Kaiqin Lao, and X. Sunney Xie 2006 "Probing Gene Expression in Live Cells, One Protein Molecule at a Time." *Science (New York, N.Y.)* 311(5767): 1600–1603.

Zare, Richard N., and Samuel Kim 2010 "Microfluidic Platforms for Single-Cell Analysis." *Annual Review of Biomedical Engineering* 12(1): 187–201.

Zhao, Yanan, Brian Ashcroft, Peiming Zhang, Hao Liu, Suman Sen, Weisi Song, JongOne Im, et al. 2014 "Single-Molecule Spectroscopy of Amino Acids and Peptides by Recognition Tunnelling." *Nature Nanotechnology* 9(6): 466–473.

Zhao, Yanan, Stuart Lindsay, Sunhwa Jeon, Hyung-Jun Kim, Liang Su, Boram Lim, and Sangho Koo 2013 "Combined Effect of Polar Substituents on the Electronic Flows in the Carotenoid Molecular Wires." *Chemistry – A European Journal* 19(33): 10832–10835.

APPENDIX A

PERMISSIONS TO USE COPYRIGHTED MATERIALS

NATURE PUBLISHING GROUP LICENSE TERMS AND CONDITIONS

Sep 23, 2016

This Agreement between kuo ("You") and Nature Publishing Group ("Nature Publishing Group") consists of your license details and the terms and conditions provided by Nature Publishing Group and Copyright Clearance Center.

License Number	3955020691361
License date	Sep 23, 2016
Licensed Content Publisher	Nature Publishing Group
Licensed Content Publication	Nature Methods
Licensed Content Title	Deep tissue two-photon microscopy
Licensed Content Author	Fritjof HelmchenandWinfried Denk
Licensed Content Date	Dec 1, 2005
Type of Use	reuse in a dissertation / thesis
Requestor type	academic/educational
Format	electronic
Portion	figures/tables/illustrations
Number of figures/tables/illustrations	1
High-res required	no
Figures	Figure 1
Author of this NPG article	no
Your reference number	
Title of your thesis / dissertation	Single Cell RT-qPCR on 3D Spheroid Cells
Expected completion date	Dec 2016
Estimated size (number of pages)	70
Requestor Location	kuo-chen wang 1249 e spence TEMPE, AZ 85281 United States Attn: kuo-chen wang
Billing Type	Invoice
Billing Address	kuo-chen wang 1249 e spence TEMPE, AZ 85281 United States Attn: kuo-chen wang
Total	0.00 USD
Terms and Conditions	